IDENTIFICATION OF HUB GENES AND miRNA ASSOCIATED WITH MERKEL CELL CARCINOMA BY INTEGRATED BIOINFORMATICS ANALYSIS

MAJOR PROJECT REPORT

SUBMITTED IN PARTIAL FULFILMENT OF THE REQUIREMENTS

FOR THE AWARD OF THE DEGREE OF

MASTER OF TECHNOLOGY

IN

BIOINFORMATICS

Submitted by

Mehak Bhatnagar

2K17/BIO/05

Under the supervision of

Dr. Yasha Hasija

Associate Professor

DEPARTMENT OF BIOTECHNOLOGY

DELHI TECHNOLOGICAL UNIVERSITY

(Formerly Delhi College of Engineering)

Bawana Road, Delhi-110042

JUNE, 2019

CANDIDATE'S DECLARATION

I, Mehak Bhatnagar, student of M.Tech Bioinformatics, 4th semester, bearing Roll No. 2K17/BIO/05, at the Department of Biotechnology, Delhi Technological University, Delhi declare that my project work titled "**Identification of hub genes and miRNA associated with Merkel Cell Carcinoma by integrated bioinformatics analysis**", is original and no part of this work report has been submitted for the fulfilment of any other degree or diploma. All the given information and work is original to my knowledge.

Date:

Place:

Mehak Bhatnagar

(2K17/BIO/05)

Department of Biotechnology

Delhi Technological University

Delhi-110042

CERTIFICATE

This is to certify that the major project entitled "Identification of hub genes and miRNA associated with Merkel Cell Carcinoma by integrated bioinformatics analysis" is the bona fide work of Ms. Mehak Bhatnagar, an M.Tech. IInd Year (Bioinformatics) student from Delhi Technological University, Delhi, and is a record of her own work carried out under my supervision and guidance. The information and data enclosed in this report is original and has not been submitted elsewhere for honouring of any other degree.

Date:

Place:

Dr. Yasha Hasija

(SUPERVISOR)

Department of Biotechnology

Delhi Technological University

Delhi-110042

Prof. Jai Gopal Sharma

Head of Department

Department of Biotechnology

Delhi Technological University

Delhi-110042

ABSTRACT

Merkel Cell Carcinoma is a highly aggressive form of non-melanoma skin cancer. Due to the rarity of the disease, MCC remains a cancer type that is yet to be fully researched. This is of immediate significance now as the incidences of MCC have been on a rise and the disease is often associated with fatality. Therefore, the purpose of this study was to explore the presence of crucial genes and miRNAs involved in Merkel Cell Carcinoma based on microarray analysis. The expression profile data of GSE39612 and GSE45146 were obtained from Gene Expression Omnibus. The differentially expressed genes (DEGs) were screened, followed by functional enrichment analysis, protein-protein interaction (PPI) network construction and analysis of significant network modules. Hub genes were identified using MCODE and cytoHubba plug-in. After the DE miRNAs were screened, their putative target genes were identified by TargetScan, miRDB and miRTarBase. The overlapped genes found between the putative targets and the DEGs were used to construct a DEG-DEmiR network in Cytoscape. Lastly, hub miRNAs present in the DEGs-DEmiR network were identified and annotated. A total of 449 DEGs were identified including 164 upregulated genes and 285 downregulated genes. DEGs were mostly enriched in epidermis development, keratinocyte differentiation, structural molecule activity, cAMP signalling pathway, calcium signalling pathway and oocyte meiosis. Using the results of MCODE and cytoHubba, 3 significant clusters were extracted from the PPI network and 16 genes (*AURKA, FLG, KIF4A, DSG1, PKP1, LOR, BUB1, CDC6, CENPE, CXCR4, FOXM1, CXCL12, CDSN, DSG3, IVL* and *DSP*) were selected as core protein-coding DEGs based upon their topological parameters. Besides, a total of 17 DEmiRs were identified, including 16 downregulated and 1 upregulated miRNA. 56 pairs of validated DEGs-DEmiRs and 221 pairs of predicted DEGs-DEmiRs were curated from miRTarBase and TargetScan & miRDB respectively. Finally, Network Analyser was used to identify the following as hub miRNA: hsa-miR-1, hsa-miR-19a, hsa-miR-9-5p, hsa-miR-9-3p, hsa-miR-454 and hsa-miR-195-3p.

Keywords Merkel Cell Carcinoma **.** Differentially expressed genes **.** Protein-protein interaction network **.** DE microRNAs

ACKNOWLEDGEMENT

I express deep gratitude to my guide Dr Yasha Hasija for her able guidance, suggestions and constructive support. I'm indebted to her for the constant support and direction at every step of the project, enabling me to gain knowledge and experiences that would be valuable forever.

Furthermore, without her valued suggestions and cooperation this project would not have taken shape. It has indeed been an enriching scientific experience and I would like to thank her for providing me an opportunity to work under her guidance.

I express my gratitude to the entire faculty for ably guiding me through the different fields of biotechnology and bioinformatics. A special thanks to them for their timely guidance throughout the course of the project. I also acknowledge the support provided by the staff of this department.

I extend a sincere acknowledgement to my colleagues and friends for their suggestions and moral support during my work.

Finally, I would like to thank my parents whose love, faith and patience in me were a constant motivating factor during this study.

Mehak Bhatnagar

(2K17/BIO/05)

TABLE OF CONTENTS

LIST OF FIGURES

LIST OF TABLES

LIST OF ABBREVIATIONS

BCC	Basal Cell Carcinoma
BH	Benjamini-Hochberg
BP	Biological Process
CC	Cellular Component
DAVID	Database for Annotation, Visualization and Integrated Discovery
DEG	Differentially Expressed Genes
DEmiR	Differentially Expressed micro RNA
EPC	Edge Percolated Component
FC	Fold Change
FDR	False Discovery Rate
GEO	Gene Expression Omnibus
GO	Gene Ontology
KEGG	Kyoto Encyclopaedia of Genes and Genomics
MCC	Merkel Cell Carcinoma
MCC	Maximal Clique Centrality
MCODE	Molecular Complex Detection
MCPyV	Merkel Cell Polyomavirus
MF	Molecular Function
MNC	Maximum Neighborhood Component
PPI	Protein-Protein Interaction
SCC	Squamous Cell Carcinoma
SEER	Surveillance, Epidemiology and End Results
STRING	Search tool for the retrieval of interacting genes/proteins

PART I
INTRODUCTION

1 INTRODUCTION

Merkel Cell Carcinoma (MCC) is an aggressive form of neuroendocrine carcinoma. It represents the 2nd highest cause of skin cancer related deaths despite being a relatively rare form of cancer (Schadendorf et al, 2017). It was described in 1972 as a trabecular carcinoma of the skin whose incidence has been gradually increasing over the years (Tokar C, 1972). A series of ultrastructural studies revealed the similarity of these cancer cells to that of Merkel Cells (a type of mechanoreceptor cells present in the skin), which led to the renaming of these cells from trabecular carcinoma to Merkel Cell Carcinoma (Tang CK and Tokar C, 1972). Different risk factors have been associated with MCC such as advancement in age, immunosuppression, and exposure to UV. A link between MCC and PyV infection has also been established. An existing, concurrent or even a previous diagnosis of Chronic Lymphocytic Leukaemia (CLL) is more frequent in people with MCC (Kaae et al, 2010). However, the exact biology of MCC and its carcinogenesis is yet to be fully explored.

The current treatments for MCC are surgery along with radiation or chemo-radiation. The first FDA approved drug for MCC was avelumab based on a clinical trial of eighty-eight patients diagnosed with metastatic MCC who had formerly undergone chemo-radiation for the same (Kaufman et al, 2016). A second drug was approved in the beginning of 2019, called pembrolizumad. Both these drugs are immune checkpoint inhibitors (Nghiem et al, 2016). As a result, there has been a complete sea change in the management of MCC patients in the last two years. Prior to using immunotherapy as a first line of treatment, MCC patients were treated just like any other individual with a neuroendocrine tumor. However, the current approval from FDA has been an accelerated one, based on promising results from a relatively small number of patients, which means that the more research and trials are undergoing currently considering the fact that a very small cohort was used for clinical trials. Although, 56% of the drug recipients have shown a positive response, many stopped using the drug due to severe side effects. A further issue is that many patients with

MCC may not be ideal candidates for immunotherapy because their immune systems have been suppressed—due to organ/graft transplantation, lymphoma or HIV (Nghiem et al, 2016).

At the moment, there are no biomarkers that could help to select patients more effectively for new therapies, and further research is crucial. The present study is therefore an attempt to identify critical genes and microRNAs in MCC by various in silico methodologies. The objectives of this study include:

- To select, process and analyse microarray datasets from GEO and identify differentially expressed genes and differentially expressed miRNAs in Merkel Cell Carcinoma.
- To determine biological terms and pathways related to DEGs (Differentially Expressed Genes).
- To construct and analyse a Protein-protein Interaction (PPI) network of DEGs to determine hub-genes.
- To construct a network describing the interaction between pairs of DEGs and DEmiRNA.
- To identify hub miRNAs and determine related biological terms for the hub nodes.

PART II
REVIEW OF LITERATURE

2 REVIEW OF LITERATURE

This section introduces the epidemiology, prognosis, pathogenesis, current therapy and unmet medical needs associated with Merkel Cell Carcinoma.

2.1 Epidemiology

2.1.1 Incidence of MCC

The incidence of MCC has exhibited a greater than three-fold increase in the past thirty years, accompanied by increase in mortality (Fitzgerald et al, 2015). A few population-wide epidemiology studies have been conducted in the US, New Zealand, Australia and a few European countries that revealed the reported local occurrence to vary between 0.1 and 0.88 per 100.000 person-years. Higher incidence rates were stated in New Zealand (Robertson, 2015) and Australia (Youlden, 2014 & Girschik, 2011) and the lowest rates in Eastern France (Riou-Gotta et al, 2009) and Scotland (Mills et al, 2006). Despite advancements in understanding of MCC biology, the 5-year survival rates still remain low (0-18%) for advanced-stage MCC (Lemos et al, 2010 & Lebbe at el, 2015).

2.1.2 Risk Factors associated with MCC

MCC risk is influenced by a multitude of patient factors that include ethnicity, age, sex, and medical history. Other factors such as UV exposure, advancement in age and immunosuppression of patients has also been associated with MCC development. According to a study performed by Albores-Saavedra, 94.9% of white patients were associated with MCC compared to a mere 4.1 % of non-white population (Albores-Saavedra et al, 2010). MCC has been diagnosed at earlier ages (Koksal et al, 2009 & Marzban et al, 2011) where it is often linked to immunosuppression in cases of organ transplantation (Kempf et al, 2013). Patients with an HIV infection and those with a maintained immunosuppression with the help of azathioprine and mTOR inhibitors were linked with an even greater chance of MCC (Lanoy et al, 2010).The chance of MCC is amplified by 1.36 times in patients

diagnosed with other tumours such as melanoma, non-Hodgkin lymphoma, multiple myeloma and chronic lymphocytic leukaemia (Howard et al, 2006).

2.2 Clinico-pathological Features

The clinical presentation of MCC tumor is of a firm, painless, reddish-violet, rapidly growing nodule that is often dome- shaped (Heath et al, 2008 & Smith et al, 2012). MCC nodules are mostly found in areas exposed by the sun such as the head and neck (Medina-Franco et al, 2001).

The AEIOU acronym has been developed to characterise the medical features linked with MCC which is expanded as asymptomatic, expanding rapidly, immune suppression, older than 50 and UV-exposed site on a person with fair skin. In a study by Heath et al, out of 195 patients 89% patients were associated with 3 or greater AEIOU indications (Heath et al, 2008).

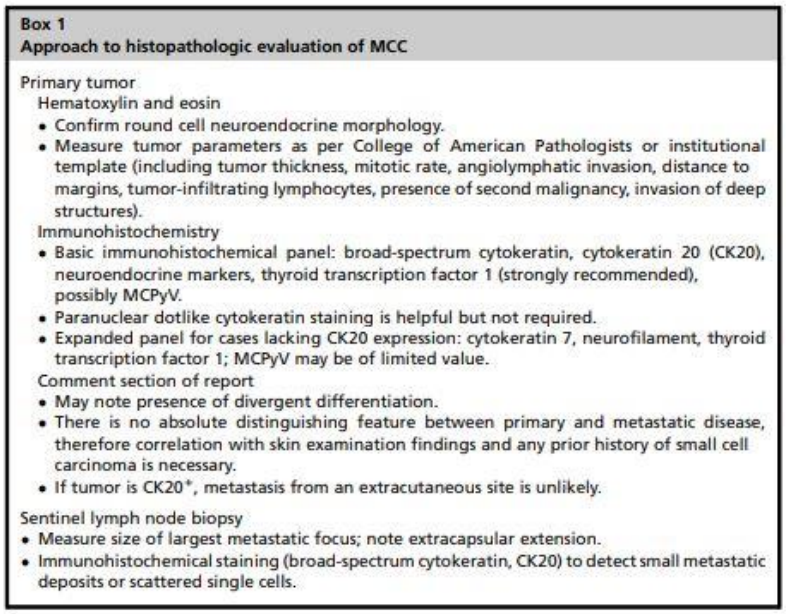

Box 1
Approach to histopathologic evaluation of MCC

Primary tumor

Hematoxylin and eosin

- Confirm round cell neuroendocrine morphology.
- Measure tumor parameters as per College of American Pathologists or institutional template (including tumor thickness, mitotic rate, angiolymphatic invasion, distance to margins, tumor-infiltrating lymphocytes, presence of second malignancy, invasion of deep structures).

Immunohistochemistry

- Basic immunohistochemical panel: broad-spectrum cytokeratin, cytokeratin 20 (CK20), neuroendocrine markers, thyroid transcription factor 1 (strongly recommended), possibly MCPyV.
- Paranuclear dotlike cytokeratin staining is helpful but not required.
- Expanded panel for cases lacking CK20 expression: cytokeratin 7, neurofilament, thyroid transcription factor 1; MCPyV may be of limited value.

Comment section of report

- May note presence of divergent differentiation.
- There is no absolute distinguishing feature between primary and metastatic disease, therefore correlation with skin examination findings and any prior history of small cell carcinoma is necessary.
- If tumor is CK20+, metastasis from an extracutaneous site is unlikely.

Sentinel lymph node biopsy

- Measure size of largest metastatic focus; note extracapsular extension.
- Immunohistochemical staining (broad-spectrum cytokeratin, CK20) to detect small metastatic deposits or scattered single cells.

Figure 2.1 A Histopathological approach to MCC evaluation

2.3 Merkel Cell Carcinoma pathogenesis

Classification of MCC is based on the infection of MCPyV, and is therefore classified as either MCPyV positive or MCPyV negative tumours. According to studies, patients with negative MCPyV tumours have worse prospects compared to

patients with MCPyV positive tumours. (Moshiri et al, 2017 & Leroux-Kozal, 2015).

2.3.1 The Merkel cell polyomavirus

In nearly 80% of the cases, MCC progression is associated with a MCPyV infection although the mechanism remains unexplained (Gonzalez-Vela et al, 2017; Liu et al, 2016; Goh et al, 2016). Since the exact cells infected by MCPyV were unknown and the virus replicated at a slow pace, the mechanism for MCC development is still not well explained (Feng et al, 2011 & Neumann et al, 2011). Two separate mechanisms were suggested to explain MCPyV infection of fibroblasts and the consequence of the infection leading to MCC tumors (Liu et al, 2016). One possibility is the transformation of the fibroblasts, after MCPyV infection, which leads to activation of genes that cause MCC tumours. The second possibility was an unintentional infection of merkel cells present close to infected fibroblasts (Fig. 2.2). This suggestion was validated by stating that the dead-end replication setting of Merkel cells favours the MCPyV integration and transformation (Liu et al, 2016).

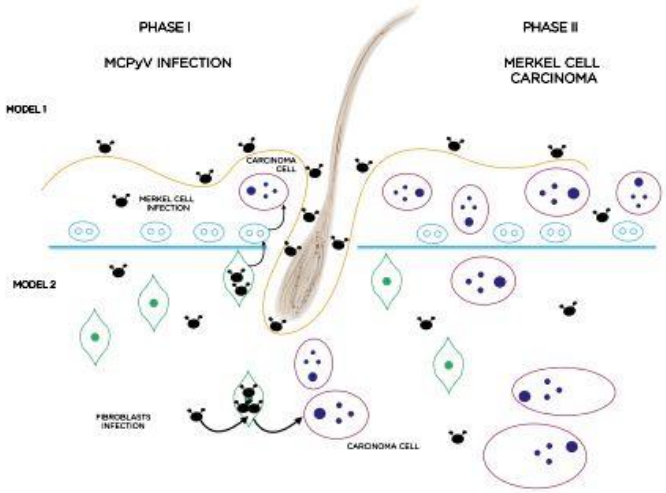

Fig. 1 Proposed models for the development of MCC based on infection by MCPyV (black figures). Phase I represents the infection with MCPyV and phase II MCC development. In model 1, the authors propose that infection of the Merkel cells occurs when there is contact with infected fibroblasts in the vicinity, since Merkel cells are post-mitotic cells that can promote viral integration and transformation. In model 2, the authors propose that MCC arises from fibroblasts that are infected by MCPyV, which in turns induces malignant transformation. Adapted from Liu W, MacDonald M, You J. Merkel cell polyomavirus infection and Merkel cell carcinoma. Current opinion in virology 2016;20:20–27 [38]. Light blue cells – Merkel cells; Black figures – MCPyV virus; Green cells – fibroblasts; Purple cells – MCC cells

Figure 2.2 Suggested models MCPyV negative MCC tumor development

2.3.2 UV radiation

UV radiation exposure is a known associate of MCC pathogenesis. MCC is prevalent in patients with light skin in comparison to patients with dark skin (Heath et al, 2008). A 95 MCC patient Australian study revealed that only 23% of the patients tested positive for MCPyV (Dabner et al, 2014). In MCPyV positive tumors the numbers of mutations are less in comparison to MCPyV negative tumors (Harms et al, 2015).

2.3.3 Immunosuppression

People with B-cell cancers, organ transplantations or HIV are at a higher risk of acquiring MCC due to immunosuppression (Engles et al, 2002 and Tadmor et al, 2011). The interface between UV radiation, MCPyV infection and immunosuppression is not yet elucidated. One theory suggests that viral replication and proliferation of atypical cells must be facilitated by immunosuppression. In addition, use of azathioprine (immunosuppressive drug) has a synergistic effect in promoting mutagenesis and carcinogenesis (Perrett et al, 2008 and Han et al, 2012).

2.4 Potential Prognostic Biomarkers

Quite a few potential prognostic biomarkers have been studied for MCC. These include tumor expression of PD-L1, proangiogenic factor expression and p63 expression (Lipson et al, 2013; Fernandes-Figuerez et al, 2007; Asioli et al, 2007). The largest prospective study of 282 MCC tumors was reported by Moshiri and colleagues, who remarked on the significantly improved outcome of MCPyV positive tumors compared to MCPyV-negative tumors (Moshiri et al, 2017). MCC tumors are often associated with a poor prognosis when an overexpression of PDGF, CD117, and PI3K is noted (Swick, 2013; Andea, 2010; Nardi, 2013). Several other biomarkers have been reported to help in prediction of disease outcomes in MCC patients such as p63, CD34 and sonic hedgehog pathway proteins (Lipson, 2013; Stetsenko et al, 2013; Brunner et al, 2010). However, substantial and inclusive data are currently deficient when it comes to assigning any biomarker to a clear prognostic association.

2.5 Clinical Trials and approved treatments

2.5.1 Immunotherapy

MCC tumors are excellent candidates for immunotherapy due to a high load of expression of neoantigens (Goh et al, 2016). In 2017, the Food and Drug Administration (FDA) approved the immunotherapy drug avelumab (Bavencio®) for the treatment MCC. It is the first FDA-approved treatment for this disease. The drug has, however, not been approved by the regulatory authorities, in Europe (Kaufmann et al, 2016).

Early this year, FDA approved another immune-checkpoint inhibitor drug called pembrolizumad for treatment of locally advanced or metastatic MCC. Objective responses were recorded for fourteen patients including four complete and ten responses that were partial. A median follow-up of thirty-three weeks revealed the relapse of only 2% of the responders (Nghiem et al, 2016).

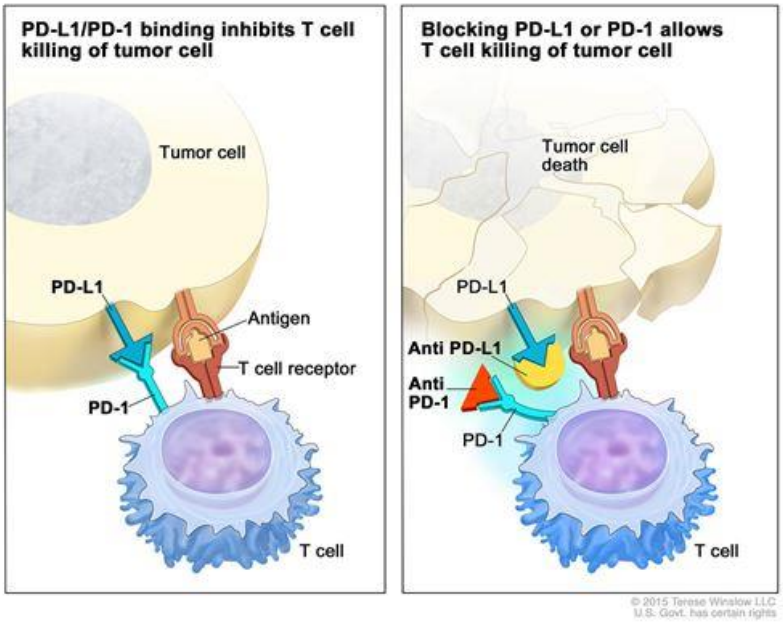

Figure 2.3 Pembrolizumab targets a protein on immune cells called PD-1, protein of the family of checkpoint proteins that restrain the immune response. (https://www.cancer.gov/news-events/cancer-currents-blog/2016/pembrolizumab-merkel-cell)

Lastly, a clinical trial for another anti-PD-1 inhibitor, nivolumab, is ongoing. So far, favourable response has been noted in two patients and further investigation about its safety, efficacy and role as a combination therapy with viral-associated tumors is currently going on. (Mantripragada et al, 2015 & Walocko et al, 2016).

NCT number	Title	Interventions	Phase
NCT02196961	Adjuvant Therapy of Completely Resected Merkel Cell Carcinoma With 3 mg/kg BW Ipilimumab (Yervoy®) Versus Observation (ADMEC)	Ipilimumab	2
NCT02514824	MLN0128 in Recurrent/Metastatic Merkel Cell Carcinoma	MLN0128	1–2
NCT02465957	QUILT-3.009: Study of aNK Infusions in Combination With ALT-803 in Patients With Stage III (IIIB) or Stage (IV) Merkel Cell Carcinoma (MCC)	aNK (NK-92)	2
NCT02155647	Avelumab in Subjects With Merkel Cell Carcinoma (JAVELIN Merkel 200)	Avelumab	2
NCT02584829	Localized Radiation Therapy or Recombinant Interferon Beta and Avelumab With or Without Cellular Adoptive Immunotherapy in Treating Patients With Metastatic Merkel Cell Carcinoma	Avelumab, MCPyV TAg-specific Polyclonal Autologous CD8-positive T Cells, RT and Recombinant Interferon Beta	1–2
NCT02819843	A Study of T-VEC (Talimogene Laherparepvec) With or Without Radiotherapy for Melanoma, Merkel Cell Carcinoma, or Other Solid Tumors	T-VEC (Talimogene Laherparepvec) and Hypofractionated Radiotherapy	2
NCT03071406	Randomized Study of Nivolumab + Ipilimumab+/− SBRT for Metastatic Merkel Cell Carcinoma	Nivolumab, ipilimumab and Stereotactic Body Radiation Therapy (SBRT)	2
NCT02351128	Treatment of Unresectable and/or Metastatic Merkel Cell Carcinoma by Somatostatin Analogues (PHRC-Merkel)	Lanreotide	2
NCT02978625	Talimogene Laherparepvec and Nivolumab in Treating Patients With Refractory Lymphomas or Advanced or Refractory Non-melanoma Skin Cancers	Nivolumab, T-VEC	2
NCT02488759	An Investigational Immuno-therapy Study to Investigate the Safety and Effectiveness of Nivolumab, and Nivolumab Combination Therapy in Virus-associated Tumors (CheckMate358)	Nivolumab, ipilimumab, BMS-986016, Daratumumab	1–2
NCT02831179	Veliparib, Capecitabine, and Temozolomide in Patients With Advanced, Metastatic, and Recurrent Neuroendocrine Tumor	Capecitabine, temozolomide and veliparib	1
NCT02936323	PEN-221 in Somatostatin Receptor 2 Expressing Advanced Cancers Including Neuroendocrine and Small Cell Lung Cancers	PEN-221	1–2
NCT02890368	Trial of Intratumoral Injections of TTI-621 in Subjects With Relapsed and Refractory Solid Tumors and Mycosis Fungoides	TTI-621	1
NCT02643303	A Phase 1/2 Study of *in Situ* Vaccination With Tremelimumab and IV Durvalumab Plus PolyICLC in Subjects With Advanced, Measurable, Biopsy-accessible Cancers	Durvalumab, Tremelimumab, Poly ICLC	1–2
NCT03071757	A Study of the Safety, Tolerability and Pharmacokinetics of ABBV-368 as a Single Agent and Combination in Subjects With Locally Advanced or Metastatic Solid Tumors	ABBV-368, nivolumab	1
NCT03000257	A Study of ABBV-181 in Participants With Advanced Solid Tumors	ABBV-181	1
NCT03126110	Phase 1/2 Study Exploring the Safety, Tolerability, and Efficacy of INCAGN01876 Combined With Immune Therapies in Advanced or Metastatic Malignancies	INCAGN01876, nivolumab, ipilimumab	1–2
NCT03074513	Atezolizumab and Bevacizumab in Rare Solid Tumors	Atezolizumab, bevacizumab	2

Figure 2.3 Current clinical trials estimating the effect of immune checkpoint inhibitors and further treatments in patients with MCC (Amaral et al, 2017).

PART III

MATERIALS/ TOOLS USED

3 MATERIALS AND TOOLS

3.1 Subio Platform Inc.

Subio Platform is integrated professional data analysis software that provides various tools for analysis of microarray, RNA-seq and other 'omics' data. The software was useful in normalizing microarray data accessed from GEO database and also for identifying differentially expressed genes from the acquired datasets. The Subio platform (Free Trial) can be accessed and downloaded from https://www.subioplatform.com/.

3.2 Gene Expression Omnibus (GEO) Database

The Gene Expression Omnibus (GEO) database is a world-wide public depository that records and freely provides high-throughput gene expression and other functional datasets. Microarray data of Merkel Cell Carcinoma was accessed and downloaded from GSE39612 and GSE45146. The homepage of the GEO website is at http://www.ncbi.nlm.nih.gov/geo/

3.3 Cytoscape 3.6.0

Cytoscape, widely used open-source software, was used for visual investigation and construction of PPI networks in this study. It offers a versatile array of tools to construct biological networks, study their interactions and compute a comprehensive set of various topological parameters using its Network Analyser plug in. The Network Analyser plug-in was used to analyse the resulting PPI network in this study.

3.4 DAVID 6.8

Database for annotation, visualization and integrated discovery or DAVID was used to measure the significance of concerned genes associated with a specific pathway, BP, MF and/or CC based on a modified Fisher's exact test. DAVID's functional annotation tool was utilised in this study and can be further accessed on https://david.ncifcrf.gov/.

3.5 STRING

STRING is a widely used database of protein-protein interactions that are both known and predicted. The data is curated from various sources including but not limited to high-throughput lab experiments, automated text-mining, genomic context predictions. A PPI network was constructed for this study using the stringApp plug-in in Cytoscape, which accesses the data from STRING database and outputs the results in form of a network. The STRING database can be viewed on https://string-db.org/ and stringApp can be downloaded from https://apps.cytoscape.org/apps/stringapp.

3.6 MCODE

Molecular Complex Detection or MCODE is a Cytoscape plug-in that is used to identify highly interconnected regions, i.e. clusters, in a network. Clusters were identified and screened in PPI networks generated in this study using the default settings of MCODE in which degree cut-off is 2, haircut setting is 'on', node score cut-off of 0.2 and a k-score value 2. The latest version of MCODE (version 1.5.1) can be downloaded from http://apps.cytoscape.org/apps/mcode.

3.7 CytoHubba

CytoHubba is a user friendly Cytoscape plug-in that allows an effective ranking of network nodes based on various network parameters. This plug-in provides various topological analysis methods which include EPC, Degree, Maximum Neighbourhood Component, Maximal Clique Centrality (MCC) EcCentricity, Betweenness, and Stress centrality that can be used to identify key genes or hub nodes in any network. The plug-in can be downloaded from http://apps.cytoscape.org/apps/cytohubba/.

3.8 Tools for identification of microRNA targets

MicroRNA targets were identified using three online resources namely, TargetScan, miRDB and miRTarBase. The former two resources are predictive while the latter identifies validated miRNA targets.

PART IV

METHODOLOGY

4 METHODOLOGY

4.1 Identification of differentially expressed hub genes involved in MCC

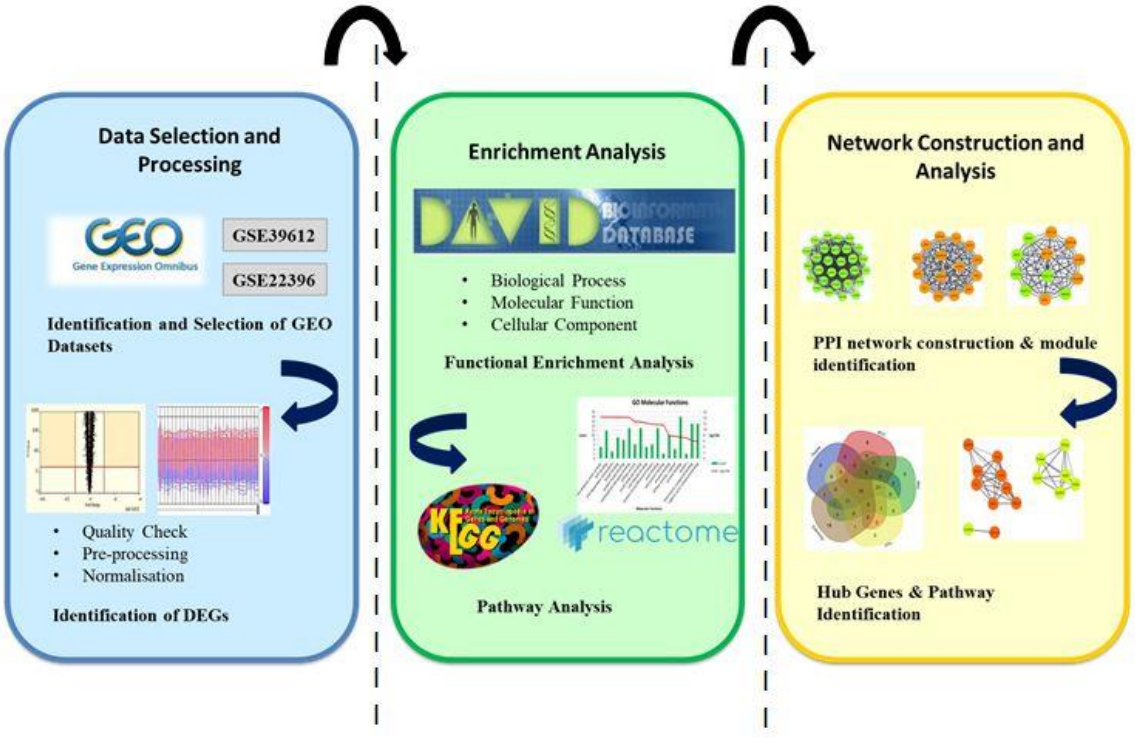

Figure 4.1 Workflow of the methodology employed to identify hub genes in Merkel Cell Carcinoma

4.1.1 Identification and selection of GEO datasets

In the present study, the expression profiles GSE39612 from the GEO database was used to carry out analysis. The series GSE39612 provides transcription data of 30 tumors from 27 different patients. This includes 19 samples of primary MCC, 11 samples of metastatic MCC, 3 samples of MCC cell lines, 4 samples of SCC, 2 samples of BCC and 64 samples of normal skin.

Disease	GEO Accession Number	Sample Size	Sample Type	Platform	Reference
Merkel Cell Carcinoma	GSE39612	19	Primary MCC	[HG-U133_Plus_2] Affymetrix Human Genome U133 Plus 2.0 Array	(Harms PW et al, 2013) PMID: 23223137
		11	Metastatic MCC		
		64	Normal Skin		

Table 4.1Microarray Dataset used in this study and its experimental design

4.1.2 Identification of differentially expressed genes (DEGs)

The quality check of the microarray was performed by plotting raw count signals from the microarray data using Subio platform. The required normalisation was then done by performing a global quantile normalization of the 90th percentile, a log transformation of base 2, lower cut-off value as 1.0 and centring of the data around the mean

Identification of DE genes was done by identifying altered expression of probes using t-tests, and BH method for multiple test corrections. Probes with expression values of $p < 0.05$ and corresponding False Discovery Rate (FDR) < 0.01 were considered to be statistically significant. A fold change (FC) value of $|FC| > 1.5$ was considered statistically significant for GSE39612.

4.1.3 Functional Enrichment Analysis

To understand the functional changes of the DEGs, their biological processes (BP), molecular function (MF) and cellular components (CC) were analysed by DAVID. A total of 449 genes which included 164 upregulated genes and 285 downregulated genes were used as the input gene set for functional enrichment. Only GO terms with p-value < 0.05 were considered statistically significant.

4.1.4 Pathway enrichment analysis

Enrichment of pathways was executed by using DAVID 6.8. The DEGs were used to perform a Fisher's exact test followed by multiple test correction using BH's False Discovery Rate correction. A corrected p-value of < 0.05 was considered statistically significant to determine the overrepresentation of certain biological pathways.

4.1.5 PPI network construction and module analysis

A PPI network was constructed using STRING database on Cytoscape. Only query proteins were displayed and a minimum required interaction score of 0.4 (medium confidence) was kept as the primary parameter. Network properties such as degree and shortest path were analysed using Network Analyser tool. Subsequently, significant module selection was done by using another Cytoscape plugin, MCODE, using their pre-set cut- off criteria.

4.1.6 DEG PPI Network Analysis to identify hub genes

Five algorithms, namely, MCC, MNC, EPC, Degree and EcCentricity were determined using cytoHubba plug-in to categorize hub genes from the PPI network. The overlapped genes of the five algorithms mentioned above were further enriched in terms of GO molecular functions, GO biological processes, GO cellular components and KEGG pathways using DAVID 6.8

4.2 Identification of differentially expressed hub microRNAs in Merkel Cell Carcinoma

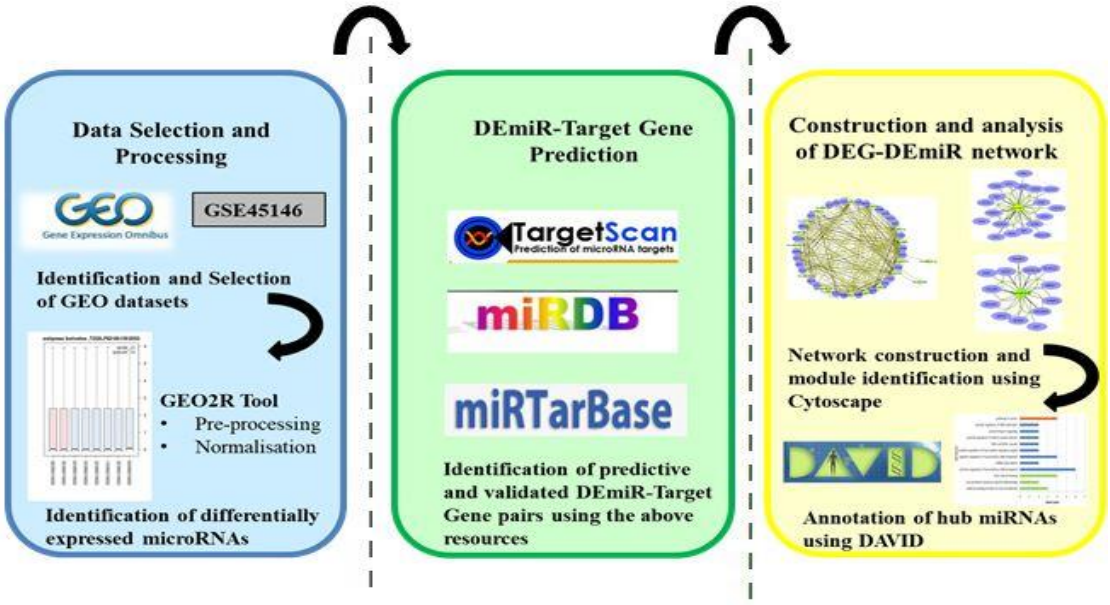

Figure 4.2 Workflow of the methodology employed to identify hub DEmiRNAs in Merkel Cell Carcinoma

4.2.1 Identification and Selection of GEO datasets

A total of 5 data series from GEO were evaluated for Merkel Cell Carcinoma microRNA using keywords, 'Merkel Cell Carcinoma', 'Homo sapiens' and 'Non-coding RNA profiling by array'. 4 data series were excluded on the basis of treatment based studies, design of the study and other dataset details. Finally, 1 data series was found suitable for the purpose of this study and was downloaded from GEO, GSE45146. Two samples from this series of normal skin and 6 samples of MCC (including both primary and metastatic tumor samples) were chosen for this study.

Disease	GEO Accession Number	Sample Size	Sample Type	Platform	Reference
Merkel Cell Carcinoma	GSE45146	2	Normal Skin	Agilent-019118 Human miRNA Microarray 2.0 G4470B (miRNA	(Renwick et al, 2013) PMID: 23728175
		6	MCC		

Table 4.2Microarray dataset used in this study and its experimental design

4.2.2 Identification of differentially expressed microRNAs

The series GSE45146 was used to identify DEmiRNAs between normal skin samples and MCC. GEO2R (http://www.ncbi.nlm.nih.gov/geo/geo2r/), an online tool that performs comparisons on GEO datasets based on the GEOquery and Limma R packages, was used to identify DEmiRNAs. The miRNAs that met the cut-off criteria of the adjusted P-value (adj. P) <0.01 and |log fold change| >1.5 were considered to be DEmiRNAs. BH method was used for multiple test corrections.

4.2.3 DE microRNA-Target Gene prediction

To identify putative target genes of the DEmiRs, three online resources were used. TargetScan Human version 7.2 (http://www.targetscan.org/vert_72/) and miRDB (http://mirdb.org/) were used to identify predictive miRNA-gene pairs while miRTarBase (http://mirtarbase.mbc.nctu.edu.tw/php/index.php) was used to identify experimentally validated miRNA-gene pairs. Individually, these were the steps performed on the sites:

TargetScan7.2

- The miRNA ID was entered and submitted.
- The "Conserved Table" was downloaded.
-

miRDB

- The option "Search by miRNA" was used and respective miRNA IDs were entered.
- The target details were noted down in a separate excel sheet.

miRTarBase

- The option “Search by miRNA was used and respective miRNA IDs were entered.
- The target details were noted down in a separate excel sheet.

4.2.4 Construction and analysis of DEG-DEmiR network

The DEGs and DEmiRs were used to construct a dysregulation network using Cytoscape. Using Network Analyser tool of Cytoscape, the above network was analysed for the purpose of finding hub miRNAs. A degree cut-off of > 20 was set as the criteria. Hub node annotation in terms of GO molecular function, GO biological process, GO cellular components and KEGG pathway were performed by DAVID 6.8.

PART V
RESULTS

5 RESULTS

5.1 Identification of differentially expressing genes (DEGs) between normal skin samples and merkel cell carcinoma (MCC)

5.1.1 Identification and selection of GEO datasets

A total of 22 data series from GEO were evaluated for Merkel Cell Carcinoma using keywords, 'Merkel Cell Carcinoma', 'Homo sapiens' and 'Expression profiling by array'. 20 data series were excluded on the basis of treatment based studies, design of the study and other dataset details. Finally, 1 data series was found suitable for the purpose of this study were downloaded from GEO, GSE39612. 64 samples of normal skin and 30 samples of MCC (including both primary and metastatic tumor samples) were chosen for this study

5.1.2 Identification of differentially expressed genes

The series GSE39612 was used to identify DEGs between normal skin samples and MCC. A global normalisation, quantile normalisation, log-transformation and centring on the mean was performed for all samples. DEGs were curated after performing student's t-test and BH correction on the data. Fold change of 1.5 and p-value < 0.05 were used to identify the DEGs. A total of 449 genes were identified which included 164 upregulated genes and 285 downregulated genes.

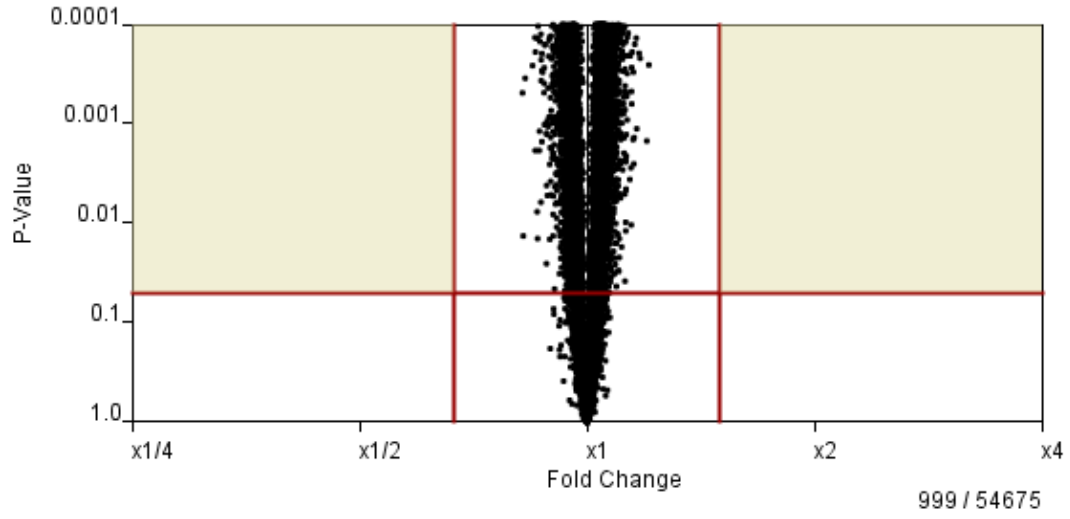

Figure 5.1Volcano Plot of GSE39612. Microarray data normalized with the 'Subio Platform'. In the X-axis, genes from middle (×1) to the left side are down-regulated while genes from middle

(×1) to the right side are up-regulated. The upside of the red line is for P value below 0.05. The up-regulated and down regulated genes with significance (P-value<0.05) were selected.

DEGs		Gene Names	Fold Change
Upregulated		NEFM	2.543639
		INSM1	2.4247596
		ISL1	2.2273529
		SNAP25	2.214575
		POU4F1	2.1981621
		TMSB15A	2.1898093
		CDH2	2.1241248
		BEX1	2.0843203
		KRT20	2.075004
		SOX11	2.070680233
Downregulated		PLA2G2A	0.66567767
		WDR1	0.6654161
		SPRR1A	0.66538364
		ZFYVE21	0.66475147
		ABHD5	0.66370875
		CAPN3	0.6636417
		PAMR1	0.66317564
		SNAP23	0.6626955
		ABCA6	0.6625355
		IL6ST	0.66252875

Figure 5.2 Differentially expressed genes (DEGs) in GSE39612. A list of few upregulated and downregulated genes in MCC. The genes are listed from largest to smallest Fold Change values.

5.1.3 Functional Enrichment Analysis

To understand the function of the DEGs, their biological processes (BP), molecular function (MF) and cellular components (CC) were analysed by DAVID. The DEGs were mainly enriched in positive regulation of transcription from RNA polymerase II promoter (GO: 0045944), oxidation-reduction process (GO: 0055114), epidermis development (GO: 0008544), keratinocyte differentiation (GO: 0030216), and positive regulation of cell proliferation (GO: 0008284) in the BP group. In CC group,

the DEGs were mostly enriched in cytoplasm (GO: 0005737), plasma membrane (GO: 0005886), extracellular exosome (GO: 0070062), integral component of plasma membrane (GO: 0005887) and extracellular space (GO: 0005615). Finally, in the MF group, the genes enriched in protein binding (GO: 0005515), calcium ion binding (GO: 0005509), protein homo-dimerization activity (GO: 0042803), structural molecule activity (GO: 0005198), transcriptional activator activity, RNA polymerase II core promoter proximal region sequence-specific binding (GO: 0001077), structural constituent of cytoskeleton (GO: 0005200), heparin binding (GO: 0008201), and iron ion binding (GO: 0005506). Only statistically significant terms, with p-values < 0.05, were considered for analysis.

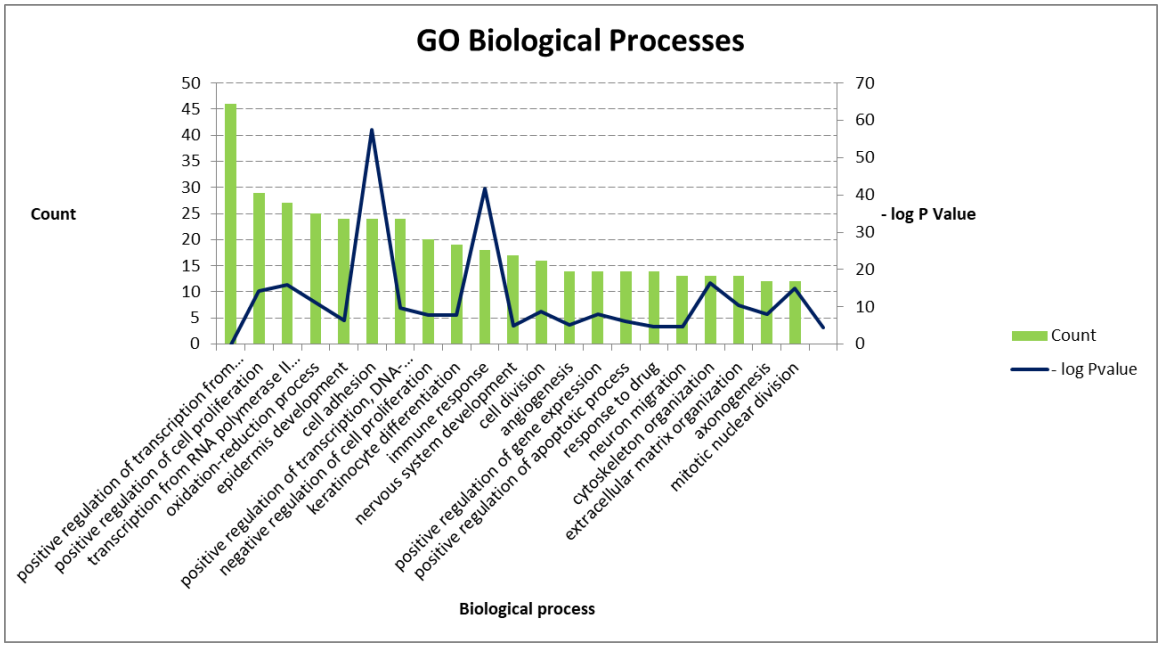

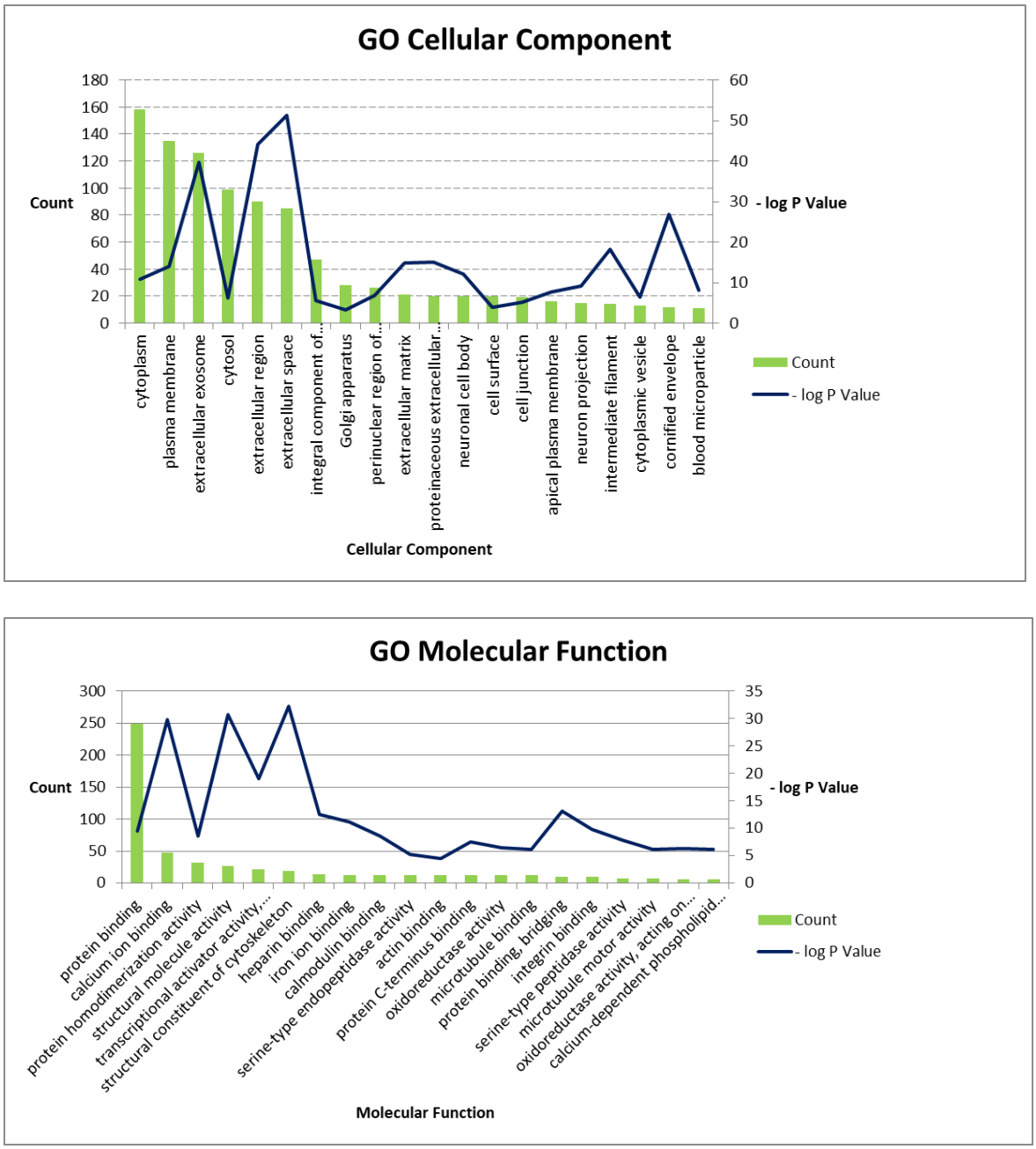

Figure 5.3 A bar graph representation of GO analysis and significantly enriched GO terms for DEGs in this dataset. GO analysis classified the DEGs into three groups (molecular function, biological process, and cellular component).

Term	Description	Count	p Value	Genes
Biological Process				
GO:0045944	positive regulation of transcription from RNA polymerase II promoter	46	4.94E-05	FGFR2, HLF, IL18, FOXM1, F2RL1, SOX2, BEX1, PAX6,
GO:0008284	positive regulation of cell proliferation	29	1.53E-05	FGFR2, KRT6A, CCK, IL6ST, FOXM1, TTK, SOX9,
GO:0006366	transcription from RNA polymerase II promoter	27	0.000471	HLF, FOXM1, SOX2, PAX6, PAX5, TP63, EHF, MYBL1,
GO:0055114	oxidation-reduction process	25	0.012791	ME1, TYRP1, HSD3B1, CYP1B1, EGLN3, BBOX1,
GO:0008544	epidermis development	24	5.00E-18	KLK7, KLK5, LCE2B, KRT31, GJB5, CDSN, SCEL,
GO:0007155	cell adhesion	24	0.001142	CLCA2, TNXB, CYP1B1, SLURP1, ADAM23, CTNND2,
GO:0045893	positive regulation of transcription, DNA-templated	24	0.004885	KLF5, SOX11, FOXM1, PSRC1, SOX2, PAX6, IGF1,
Cellular Components				
GO:0005737	Cytoplasm	158	0.000572	PALMD, DCN, KRT5, NCAPG, HJURP, POU2F3,
GO:0005886	plasma membrane	135	5.74E-05	TBC1D30, FCER1A, KLF5, VAV3, ADAM23, IL1RN,
GO:0070062	extracellular exosome	126	1.19E-12	CLEC3B, FBLN5, SPRR1B, AOX1, DSC2, DSC1, CP,
GO:0005829	Cytosol	99	0.014265	CENPE, CAPN3, RGS13, SCGN, AOX1, RAB38, HPGD
GO:0005576	extracellular region	90	5.16E-14	SCGN, OMD, FBLN1, CD55, CCL14, NPY, SFRP1..
GO:0005615	extracellular space	85	3.42E-16	FBLN1, OMD, CCL14, NPY, SFRP1, CLEC3B, FBLN5,
GO:0005887	integral component of plasma membrane	47	0.022283	P2RY14, NTRK2, KCNH6, CLDN1, PDGFRA, TM4SF1,
GO:0005794	Golgi apparatus	28	0.098523	NPY, DUSP26, ATP8A2, RAB38, PERP, KIF20A..
Molecular Function				
GO:0005515	protein binding	249	0.001438	KIF18A, CENPF, DPYSL4, CENPE, DACH1, ISL1,
GO:0005509	calcium ion binding	48	1.12E-09	DSC2, LRP8, DSC1, NCAN, DST, PROS1, CACNA1A..
GO:0042803	protein homo-dimerization activity	32	0.002538	FBLN5, KCNN2, NTRK2, PDGFRA, CLIP1, CRYBA2,
GO:0005198	structural molecule activity	27	5.44E-10	KRT15, KRT14, CLDN1, DSP, CSTA, ADD2..
GO:0001077	transcriptional activator activity, RNA polymerase II core promoter	21	1.84E-06	POU4F2, POU3F2, ZNF750, POU4F1, KLF4, PITX2..
GO:0005200	structural constituent of cytoskeleton	19	2.10E-10	KRT14, DSP, ACTL6B, NEFH, KRT2, NEFL, NEFM..
GO:0008201	heparin binding	14	0.000178	FGFR2, TNXB, ECM2, GREM2, APLP1, PRELP,

Table 5.1 A tabular representation of analysis of significant enrichment GO terms of DEGs present in MCC

5.1.4 Pathway enrichment analysis

The gene set of 449 DEGs was used to identify statistically significant pathways with p-value < 0.05. Significantly enriched pathways highlighted were cAMP signaling pathway (hsa04024), Calcium signaling pathway (hsa04020), Amoebiasis (hsa05146), Oocyte meiosis (hsa04114), Arachidonic acid metabolism (hsa00590), Glioma (hsa05214), Inflammatory mediator regulation of TRP channels (hsa04750), Vascular smooth muscle contraction (hsa04270), p53 signaling pathway (hsa04115), Aldosterone synthesis and secretion (hsa04925), GnRH signaling pathway (hsa04912) and HIF-1 signaling pathway (hsa04066).

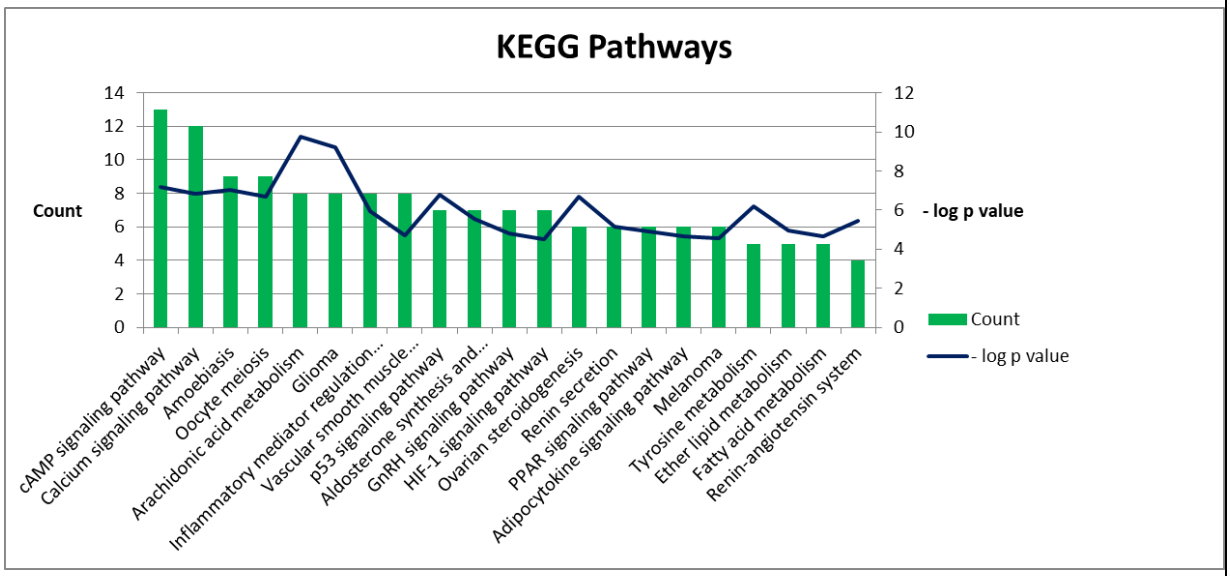

Figure 5.4 A bar graph representation of significantly enriched pathways for DEGs in this dataset

Term	Description	P-Value	Genes
hsa04024	cAMP signaling pathway	0.006951985	ATP2B2, ADCY1, PLD1, VAV3, NPY, CALML3, PLN,
hsa04020	Calcium signaling pathway	0.008673811	EGFR, GNAL, ATP2B2, AGTR1, ADCY1, CALML3, PLN,
hsa05146	Amoebiasis	0.007513759	GNAL, IL1R2, ARG1, LAMB4, ADCY1, SERPINB2,
hsa04114	Oocyte meiosis	0.009824526	CCNE2, ADCY1, CALML3, BUB1, FBXO5, IGF1, AURKA,
hsa00590	Arachidonic acid metabolism	0.001161382	AKR1C3, PLA2G4A, PTGIS, ALOX15B, PLA2G2A, EPHX2,
hsa05214	Glioma	0.001693434	EGFR, CDKN2A, CALML3, PDGFRA, IGF1, CAMK2B,
hsa04750	Inflammatory mediator regulation of TRP channels	0.016071416	ADCY1, PLA2G4A, CALML3, F2RL1, IGF1, CAMK2B,
hsa04270	Vascular smooth muscle contraction	0.037827198	ACTG2, AGTR1, ADCY1, PLA2G4A, CALML3, CALD1,
hsa04115	p53 signaling pathway	0.008943032	CCNE2, CDKN2A, RRM2, RPRM, IGF1, PERP, GTSE1
hsa04925	Aldosterone synthesis and secretion	0.021401112	AGTR1, ADCY1, HSD3B1, CALML3, CAMK2B, CALML5,
hsa04912	GnRH signaling pathway	0.035359873	EGFR, ADCY1, PLA2G4A, PLD1, CALML3, CAMK2B,
hsa04066	HIF-1 signaling pathway	0.044130154	EGFR, TF, EGLN3, ENO2, IGF1, CAMK2B, PIK3R1
hsa04913	Ovarian steroidogenesis	0.009751094	AKR1C3, ADCY1, PLA2G4A, HSD3B1, CYP1B1, IGF1
hsa04924	Renin secretion	0.028291683	AGTR1, CLCA2, CLCA4, CALML3, CALML5, AQP1
hsa03320	PPAR signaling pathway	0.033623759	CPT1B, SCD5, FABP7, ADIPOQ, ACSL6, ACSBG1
hsa04920	Adipocytokine signaling pathway	0.039542173	CPT1B, NPY, LEPR, ADIPOQ, ACSL6, ACSBG1
hsa05218	Melanoma	0.041647285	EGFR, CDKN2A, PDGFRA, IGF1, CDH1, PIK3R1
hsa00350	Tyrosine metabolism	0.013828406	DCT, TYRP1, AOX1, ADH1B, ALDH3B2
hsa00565	Ether lipid metabolism	0.032014452	PLA2G4A, PLD1, PLA2G2A, PAFAH1B1, PLPP3
hsa01212	Fatty acid metabolism	0.039315876	CPT1B, ELOVL2, SCD5, ACSL6, ACSBG1
hsa04614	Renin-angiotensin system	0.022816032	AGTR1, CPA3, CMA1, CTSG

Table 5.2 A tabular representation of significant KEGG pathways identified for the DEGs in this dataset Terms with p-value < 0.05 were considered as significant.

5.1.5 PPI network construction and module analysis

A protein-protein interaction network was constructed using STRING database on Cytoscape. Only query proteins were displayed and a minimum required interaction score of 0.4 (medium confidence) was kept as the primary parameter. A network of

448 nodes and 2190 edges were included in the DEGs network. The network consisted of 38 isolated nodes. The following network properties of degree distribution, average neighbourhood connectivity, average aggregation coefficient and distribution of shortest path were also analysed as seen in Figure 7 (a-d).

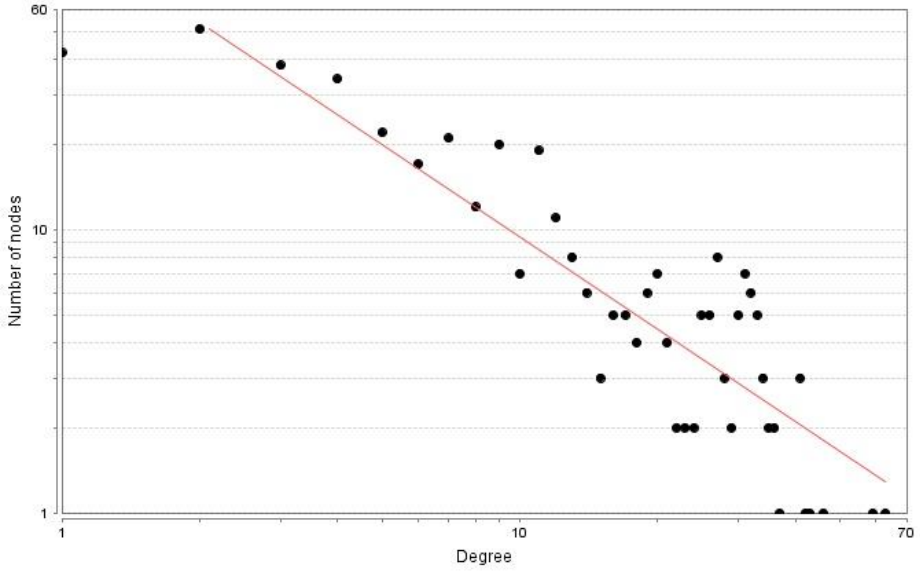

a)

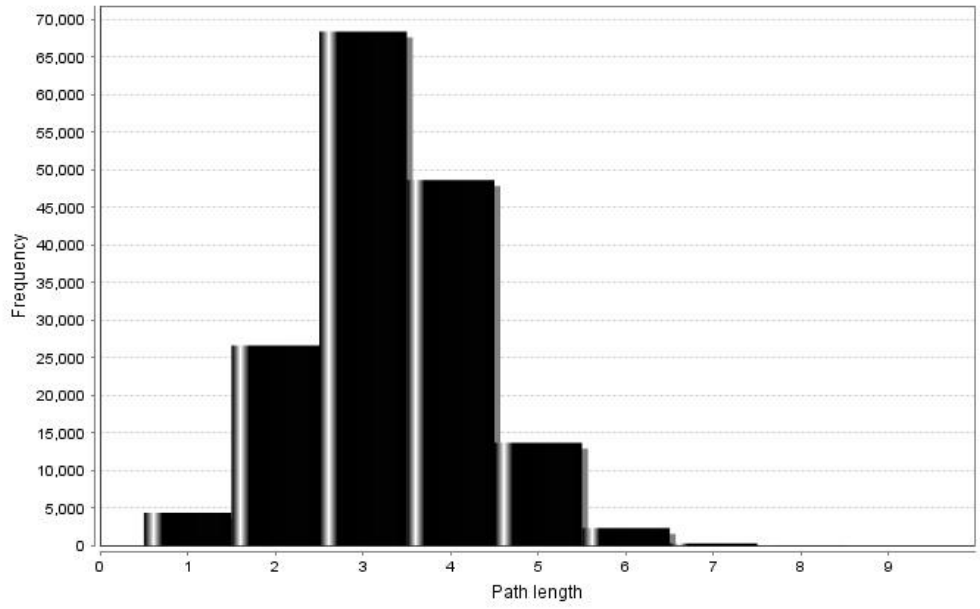

b)

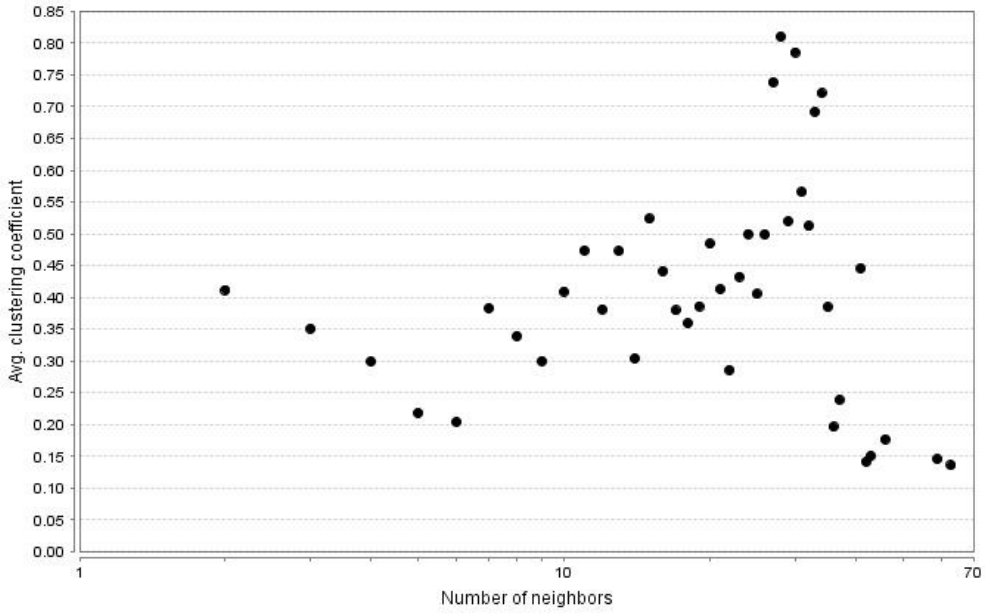

c)

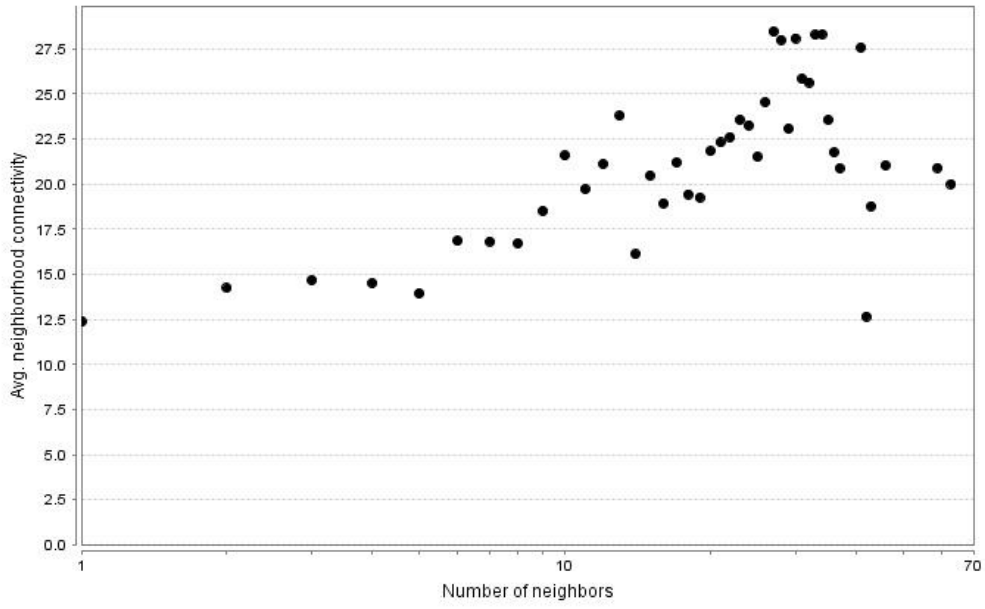

d)

Figure 5.5PPI network analysis of DEGs for characteristics of small-world network a) Distribution of degrees b) Distribution of shortest path c) average aggregation coefficient d) average neighbourhood connectivity.

Subsequently, significant module selection was done by using another Cytoscape plugin, MCODE, using their pre-set cut- off criteria. These criteria included a degree cut-off of 2, cluster finding algorithm of 'haircut', node score cut-off of 0.2, k-core value of 2 and maximum depth value of 100. As per these criteria, a total of 17 clusters were identified with an average MCODE score of 6.651. Consequently, three significant modules were selected, Cluster A with score = 28.07, nodes = 29, edges =

393; Cluster B with score = 15, nodes = 15, edges = 105; Cluster C with score = 12, nodes = 12, edges = 66.

i. Cluster A analysis

Cluster A was selected as the most significant module with an MCODE score of 28.07, nodes = 29 and edges = 393. The 29 genes included in this module are as follows: NEK2, TTK, DTL, DLGAP5, HJURP, RRM2, ASPM, BUB1, KIF20A, CENPM, FOXM1, CDC6, CCNE2, AURKA, DEPDC1, CENPF, CENPE, FBXO5, NDC80, NCAPG, HMMR, CENPA, KIF14, BUB1B, TOP2A, SPC25, KIF4A, GTSE1, and KIF18A. All of these genes were upregulated.

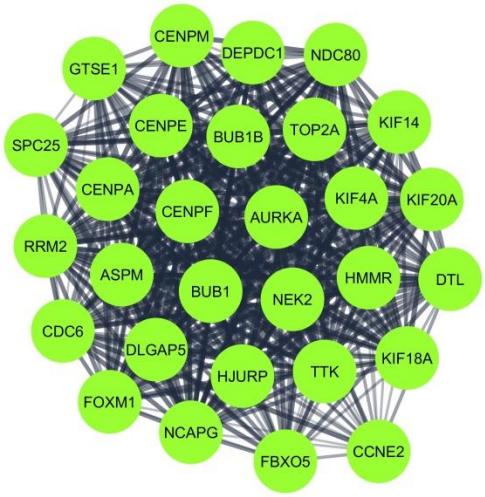

Figure 5.6 Cluster A: A significant module selected from the PPI network. The green circular nodes represent upregulated genes

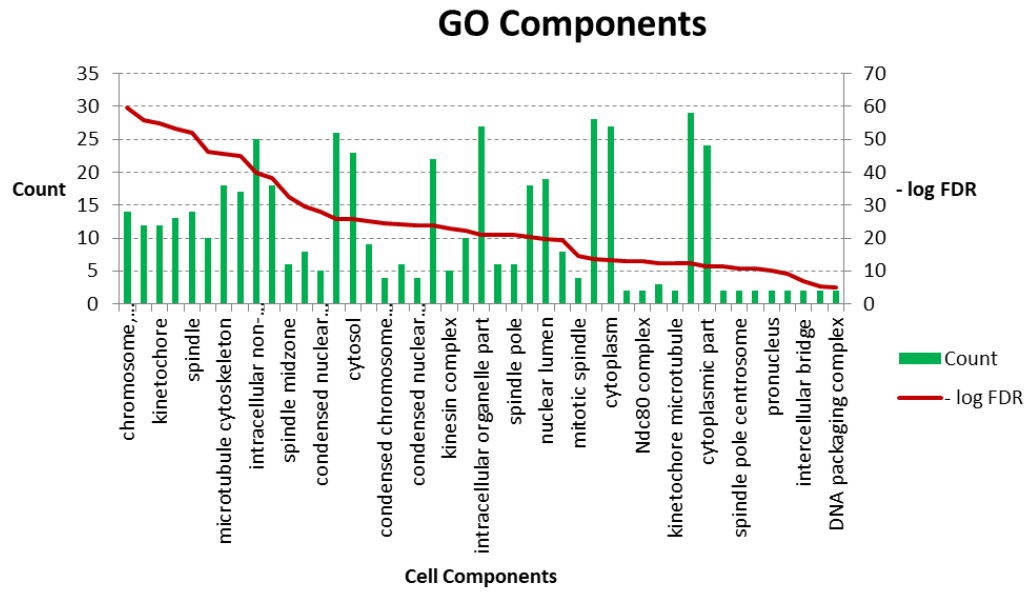
GO Components
Count
- log FDR
chromosome,...
kinetochore
spindle
microtubule cytoskeleton
intracellular non-...
spindle midzone
condensed nuclear...
cytosol
condensed chromosome...
condensed nuclear...
kinesin complex
intracellular organelle part
spindle pole
nuclear lumen
mitotic spindle
cytoplasm
Ndc80 complex
kinetochore microtubule
cytoplasmic part
spindle pole centrosome
pronucleus
intercellular bridge
DNA packaging complex
Count
- log FDR
Cell Components

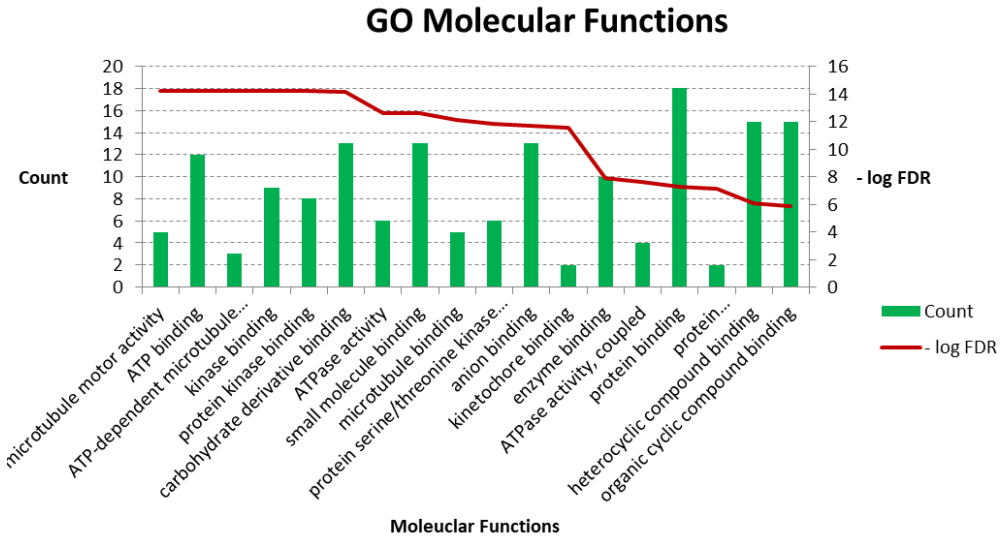
GO Molecular Functions
Count
- log FDR
microtubule motor activity
ATP binding
ATP-dependent microtubule...
kinase binding
protein kinase binding
carbohydrate derivative binding
ATPase activity
small molecule binding
microtubule binding
protein serine/threonine kinase...
anion binding
kinetochore binding
enzyme binding
ATPase activity, coupled
protein binding
protein...
heterocyclic compound binding
organic cyclic compound binding
Count
- log FDR
Moleuclar Functions

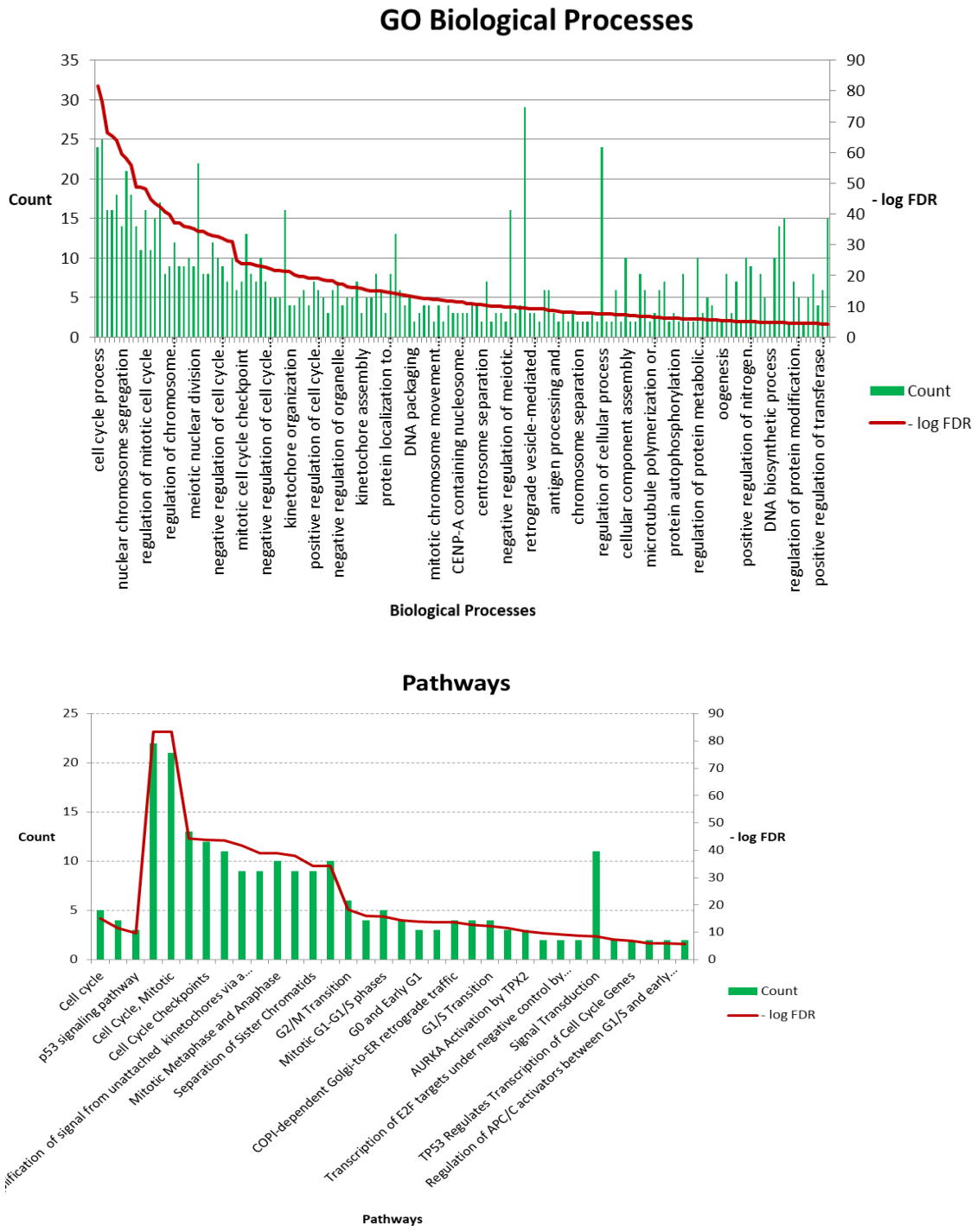

Figure 5.7 A bar graph representation of GO analysis depicting significantly enriched GO terms and pathways for DEGs in Cluster A. GO analysis classified the DEGs into three groups (molecular function, biological process, and cellular component).

This cluster was indicative of pathways enriched in cell cycle (hsa041100), p53 signalling pathway (hsa04115), cell cycle checkpoints (HAS-69620), Amplification of signal from unattached kinetochores via a MAD2 inhibitory signal (HSA-141444), Mitotic Metaphase and Anaphase (HSA-2555396) and RHO GTPase Effectors

(HSA-195258). For the biological processes group, the genes were primarily enriched in mitotic cell cycle process (GO.1903047), cell cycle (GO.0007049), regulation of cell cycle (GO.0051726), chromosome organization (GO.0051276), microtubule cytoskeleton organization (GO.0000226) and organelle localization (GO.0051640). In the MF group, ATP binding (GO.0005524), carbohydrate derivative binding (GO.0097367), anion binding (GO.0043168) and protein binding (GO.0005515) were primarily highlighted. In the CC group, the genes mainly enriched were intracellular non-membrane-bounded organelle (GO.0043232), nucleus (GO.0005634), cytosol (GO.0005829), kinetochore microtubule (GO.0005828) and also cytoplasmic part (GO.0044444).

ii. Cluster B Analysis

Cluster B was selected as the second most significant module with an MCODE score of 15, nodes = 15 and edges = 105. The 15 genes included in this module are as follows: PPL, FLG, DSG3, DSG1, TCHH, SPRR1B, DSP, DSC2, SPRR1A, DSC1, IVL, CSTA, PKP1, LOR and CDSN. All of these genes were downregulated.

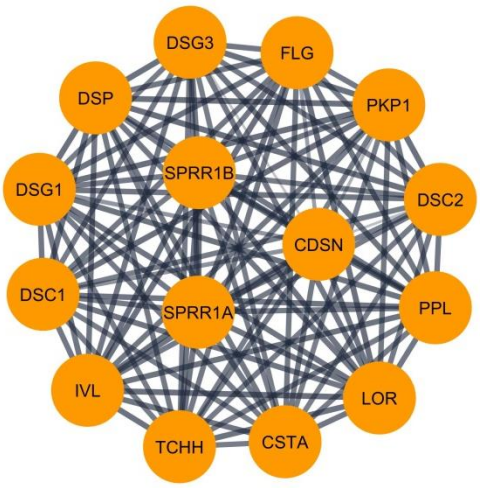

Figure 5.8 Cluster B: A significant module selected from the PPI network. The circular orange nodes represent downregulated genes

The enriched terms primarily highlighted in this module were cornification, cell-cell adhesion, structural molecule activity, protein binding, bridging and structural constituent of epidermis. The cellular components included cornified envelope,

desmosome, ficolin-1-rich granule membrane and cytosol. The key pathways emphasised were formation of the cornified envelope and immune system.

Terms	Description	Count	FDR Value	Genes
Biological Processes				
GO.0070268	Cornification	15	1.73E-31	DSG3 DSG1 DSC1 PKP1 CSTA DSC2..
GO.0018149	peptide cross-linking	7	5.03E-13	CSTA SPRR1B LOR SPRR1A IVL FLG DSP
GO.0098609	cell-cell adhesion	8	4.04E-09	DSG3 DSG1 DSC1 PKP1 CSTA DSC2
GO.0007156	homophilic cell adhesion via plasma	4	0.0000643	DSG3 DSG1 DSC1 DSC2
GO.0086073	bundle of His cell-Purkinje myocyte	2	0.00016	DSC2 DSP
GO.0098911	regulation of ventricular cardiac muscle cell	2	0.00069	DSC2 DSP
GO.0045109	intermediate filament organization	2	0.0013	PKP1 DSP
GO.0043312	neutrophil degranulation	4	0.0032	DSG1 DSC1 PKP1 DSP
GO.0086091	regulation of heart rate by cardiac conduction	2	0.0032	DSC2 DSP
GO.0007010	cytoskeleton organization	4	0.0211	PKP1 PPL LOR DSP
GO.0045216	cell-cell junction organization	2	0.0285	DSG1 DSP
Cellular Components				
GO.0001533	cornified envelope	15	2.53E-35	DSG3 DSG1 DSC1 PKP1 CSTA DSC2..
GO.0030057	Desmosome	8	7.04E-18	DSG3 DSG1 DSC1 PKP1 DSC2 PPL CDSN
GO.0101003	ficolin-1-rich granule membrane	4	1.78E-06	DSG1 DSC1 PKP1 DSP
GO.0101002	ficolin-1-rich granule	4	0.0000833	DSG1 DSC1 PKP1 DSP
GO.0044444	cytoplasmic part	14	0.0018	DSG3 DSG1 DSC1 PKP1 CSTA DSC2
GO.0005882	intermediate filament	3	0.0025	PKP1 FLG DSP
HSA-168256	Immune System	5	0.0141	DSG1 DSC1 PKP1 PPL DSP

Terms	Description	Count	FDR Value	Genes
GO.0014704	intercalated disc	2	0.004	DSC2 DSP
GO.0005829	Cytosol	10	0.0045	DSG3 DSG1 CSTA SPRR1B PPL LOR
GO.0005913	cell-cell adherens junction	2	0.0064	DSC2 DSP
GO.0005856	Cytoskeleton	6	0.0115	PKP1 PPL IVL FLG DSP TCHH
Molecular Function				
GO.0005198	structural molecule activity	9	1.25E-08	PKP1 CSTA SPRR1B PPL LOR SPRR1A IVL..
GO.0030280	structural constituent of epidermis	4	1.32E-08	PKP1 LOR SPRR1A FLG
GO.0030674	protein binding, bridging	6	4.38E-08	CSTA SPRR1B LOR SPRR1A IVL DSP
GO.0005509	calcium ion binding	6	0.0000635	DSG3 DSG1 DSC1 DSC2 FLG TCHH
GO.0086083	cell adhesive protein binding involved in	2	0.0000746	DSC2 DSP
GO.0005200	structural constituent of cytoskeleton	3	0.00035	PPL LOR DSP
GO.0005488	Binding	14	0.0213	DSG3 DSG1 DSC1 PKP1 CSTA DSC2
GO.0005515	protein binding	10	0.0306	DSG1 PKP1 CSTA DSC2 SPRR1B LOR
Pathways				
hsa05412	Arrhythmogenic right ventricular	2	0.0029	DSC2 DSP
HSA-6809371	Formation of the cornified envelope	15	5.48E-32	DSG3 DSG1 DSC1 PKP1 CSTA DSC2 SPRR1B..
HSA-351906	Apoptotic cleavage of cell adhesion proteins	4	9.84E-10	DSG3 DSG1 PKP1 DSP
HSA-6798695	Neutrophil degranulation	4	0.00055	DSG1 DSC1 PKP1 DSP

Table 5.3 A tabular representation of significantly enriched GO terms and pathways highlighted in Cluster B

iii. Cluster C analysis

Cluster C was selected as the third most significant module with an MCODE score of 12, nodes = 12 and edges = 66. The 12 genes included in this module are as follows: CCL27, GNG4, CNR1, HCAR2, NPY, LPAR1, GAL, NPY1R, ADCY1, CXCL12, CXCR4 and P2RY14.

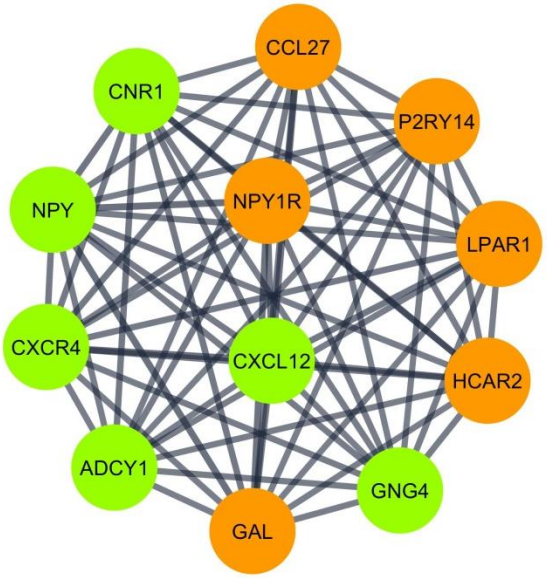

Figure 5.9 Cluster C: A significant module selected from the PPI network. The circular green nodes represent upregulated genes while the circular green nodes represent downregulated genes.

The primary pathways highlighted in this cluster were Chemokine signalling, pathway, cAMP signaling pathway, Regulation of lipolysis in adipocytes, Pathways in cancer, Neuroactive ligand-receptor interaction, Retrograde endocannabinoid signalling, Rap1 signaling pathway, Cytokine-cytokine receptor interaction, G alpha (i) signalling events, GPCR ligand binding, Class A/1 (Rhodopsin-like receptors), Peptide ligand-binding receptors and Chemokine receptors bind chemokines

Terms	Description	Count	FDR Value	Genes
Biological Processes				
GO.0007186	G protein-coupled receptor signaling	12	4.17E-12	CCL27 GAL ADCY1 P2RY14
GO.0007187	G protein-coupled receptor signaling	5	2.96E-05	ADCY1 NPY1R CNR1 LPAR1 NPY
GO.0007610	Behaviour	6	5.41E-05	GAL ADCY1 NPY1R CNR1
GO.0007188	adenylate cyclase-modulating G	4	0.00041	ADCY1 NPY1R CNR1 LPAR1
GO.0060326	cell chemotaxis	4	0.00041	CCL27 LPAR1 CXCL12 CXCR4
GO.0010646	regulation of cell communication	9	0.0012	CCL27 GAL CNR1 LPAR1 HCAR2
GO.0023051	regulation of signalling	9	0.0012	CCL27 GAL CNR1 LPAR1 HCAR2
GO.0031175	neuron projection development	5	0.0012	ADCY1 CNR1 CXCL12 NPY
GO.0065008	regulation of biological quality	9	0.0012	GAL ADCY1 NPY1R CNR1
GO.0120036	plasma membrane bounded cell	6	0.0012	ADCY1 CNR1 LPAR1 CXCL12
Cellular Components				
GO.0005886	plasma membrane	9	0.035	ADCY1 P2RY14 NPY1R CNR1
GO.0044459	plasma membrane part	7	0.035	ADCY1 P2RY14 NPY1R CNR1
GO.0005887	integral component of	5	0.0395	ADCY1 P2RY14 NPY1R CNR1

Molecular Functions				
GO.0004930	G protein-coupled receptor activity	8	4.68E-07	GAL P2RY14 NPY1R CNR1
GO.0001664	G protein-coupled receptor binding	4	0.00037	CCL27 GAL CXCL12 NPY
GO.0008528	G protein-coupled peptide receptor	3	0.0012	GAL NPY1R CXCR4
GO.0048018	receptor ligand activity	4	0.0017	CCL27 GAL CXCL12 NPY
GO.0005184	neuropeptide hormone activity	2	0.0019	GAL NPY
GO.0008009	chemokine activity	2	0.0039	CCL27 CXCL12
GO.0008188	neuropeptide receptor activity	2	0.0039	GAL NPY1R
Pathways				
hsa04062	Chemokine signaling pathway	5	3.41E-06	CCL27 ADCY1 GNG4 CXCL12
hsa04024	cAMP signaling pathway	4	0.00015	ADCY1 NPY1R HCAR2 NPY
hsa04923	Regulation of lipolysis in	3	0.00015	ADCY1 NPY1R NPY
hsa05200	Pathways in cancer	5	0.00015	ADCY1 LPAR1 GNG4 CXCL12
hsa04080	Neuroactive ligand-receptor	4	0.00022	P2RY14 NPY1R CNR1 LPAR1
hsa04723	Retrograde endocannabinoid	3	0.00097	ADCY1 CNR1 GNG4
hsa04015	Rap1 signaling pathway	3	0.0021	ADCY1 CNR1 LPAR1
hsa04060	Cytokine-cytokine receptor	3	0.0034	CCL27 CXCL12 CXCR4
HSA-418594	G alpha (i) signalling events	12	4.10E-19	CCL27 GAL ADCY1 P2RY14
HSA-500792	GPCR ligand binding	11	5.11E-16	CCL27 GAL P2RY14 NPY1R
HSA-373076	Class A/1 (Rhodopsin-like	10	2.45E-15	CCL27 GAL P2RY14 NPY1R
HSA-375276	Peptide ligand-binding receptors	6	8.84E-09	CCL27 GAL NPY1R CXCL12
HSA-380108	Chemokine receptors bind	3	4.23E-05	CCL27 CXCL12 CXCR4

Table 5.4 Significantly enriched GO terms and pathways highlighted in Cluster C

5.1.6 Identification of Hub Genes and Pathways through DEG PPI Network Analysis

The cytoHubba application was employed to identify the top 10 genes evaluated using the following algorithms: Degree, MCC, MNC, EPC and EcCentricity as given in Table 7.

Degree	Gene	MCC	Gene	MNC	Gene	EPC	Gene	EcCentricity	Gene
63	EGFR	9.22E+13	AURKA	59	EGFR	91.987	CHD1	0.18125	CDH1
59	CDH1	9.22E+13	FOXM1	56	CDH1	91.132	EGFR	0.18125	EGFR
46	SOX2	9.22E+13	ASPM	42	SOX2	90.78	AURKA	0.18125	AURKA
43	IGF1	9.22E+13	CENPF	41	KRT5	90.639	FOXM1	0.18125	FOXM1
42	SNAP25	9.22E+13	CENPE	40	IGF1	87.4	CDC6	0.18125	SOX2
41	AURKA	9.22E+13	BUB1	39	AURKA	87.208	BUB1	0.18125	KRT5
41	KRT5	9.22E+13	BUB1B	38	FOXM1	87.186	CENPE	0.18125	CDKN2A
41	FOXM1	9.22E+13	DLGAP5	38	SNAP25	86.817	KIF4A	0.18125	KRT14
37	CXCR4	9.22E+13	CDC6	35	CXCR4	86.711	CENPF	0.18125	LOR
36	SOX9	9.22E+13	KIF4A	34	LOR	86.388	CENPA	0.18125	NCAM1

Table 5.5 Top 10 genes evaluated in the PPI network using five calculation methods (MCC, MNC, Degree, EPC, and EcCentricity) and employing CytoHubba in Cytoscape.

Furthermore, an online tool (http://bioinformatics.psb.ugent.be/webtools/Venn/) was employed to observe the intersection of five algorithms (degree, MCC, MNC, EPC and EcCentricity) to identify the hub genes present in the network. As seen from figure 5.10, 16 genes were found in the intersection of the five algorithms. These genes include: AURKA, FLG, KIF4A, DSG1, PKP1, LOR, BUB1, CDC6, CENPE, CXCR4, FOXM1, CXCL12, CDSN, DSG3, IVL and DSP.

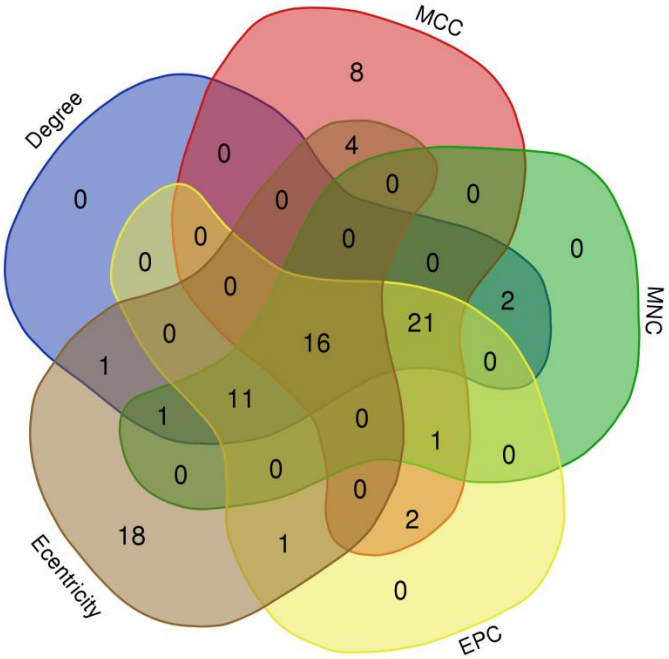

Figure 5.10 Employing an online resource, five intersecting algorithms to generate a Venn plot to identify significant hub genes. Areas with different colours correspond to different algorithms. The cross areas indicate the commonly accumulated DEGs. The elements in concurrent areas are the 16 hub genes (AURKA, FLG, KIF4A, DSG1, PKP1, LOR, BUB1, CDC6, CENPE, CXCR4, FOXM1, CXCL12, CDSN, DSG3, IVL and DSP).

The 16 hubs genes included 7 upregulated and 9 downregulated genes and were used to construct a network with 16 nodes and 34 edges. A network of these 16 hub genes revealed that the upregulated and downregulated genes were part of two individual clusters, as shown in Figure 5. A STRING enrichment analysis (GO components, GO processes, GO functions, KEGG pathways and Reactome pathways) was performed for the hub genes, keeping the FDR < 0.05. In the GO components group, the genes were mostly enriched in cornified envelope (GO.0001533), desmosome (GO.0030057), cytoskeletal part (GO.0044430), plasma membrane (GO.0005886) and cytosol (GO.0005829). In the GO process group, most genes were enriched in programmed cell death (GO.0012501), cell differentiation (GO.0030154), cornification (GO.0070268), anatomical structure development (GO.0048856), animal organ development (GO.0048513) and system development (GO.0048731). Further, genes were mainly enriched in protein binding (GO.0005515) and binding (GO.0005488) in the GO functions group. For pathway enrichment, results from both

KEGG and Reactome were considered. A cut-off value of 2 and FDR < 0.05 was considered statistically significant. Eight KEGG pathways were highlighted which included Intestinal immune network for IgA production (hsa04672), Cell cycle (hsa04110), Oocyte meiosis (hsa04114), Leukocyte trans-endothelial migration (hsa04670), Progesterone-mediated oocyte maturation (hsa04914), Chemokine signaling pathway (hsa04062), Axon guidance (hsa04360) and Cytokine-cytokine receptor interaction (hsa04060). On the other hand, reactome highlighted eighteen pathways, with the same statistical conditions intact. The major pathways highlighted were formation of the cornified envelope (HSA-6809371), developmental biology (HSA-1266738), immune system (HSA-168256) and cell cycle, mitotic (HSA-69278).

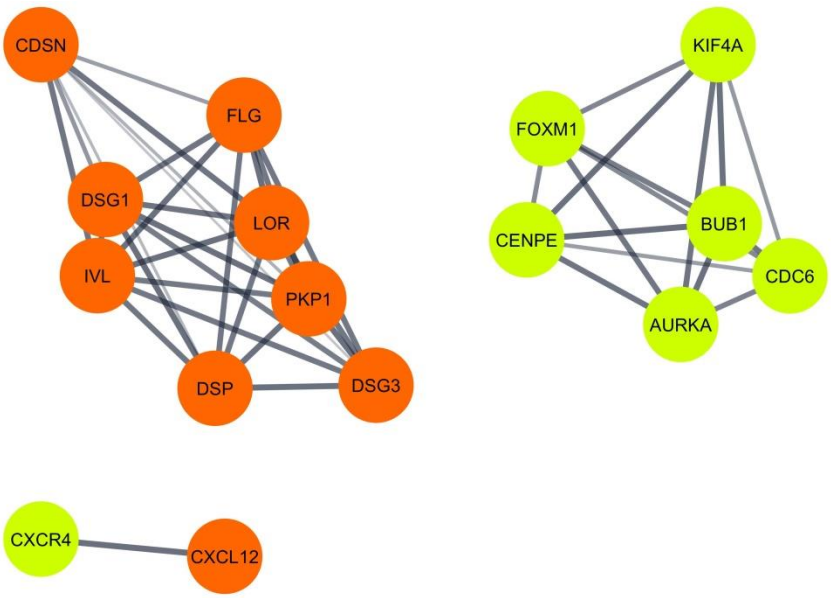

Figure 5.11 PPI Network of the hub genes with 16 nodes and 34 edges. The 16 hub genes were used to construct a network using STRING database in Cytoscape. The 'green' nodes indicate the upregulated genes while the 'red' nodes indicate the downregulated genes.

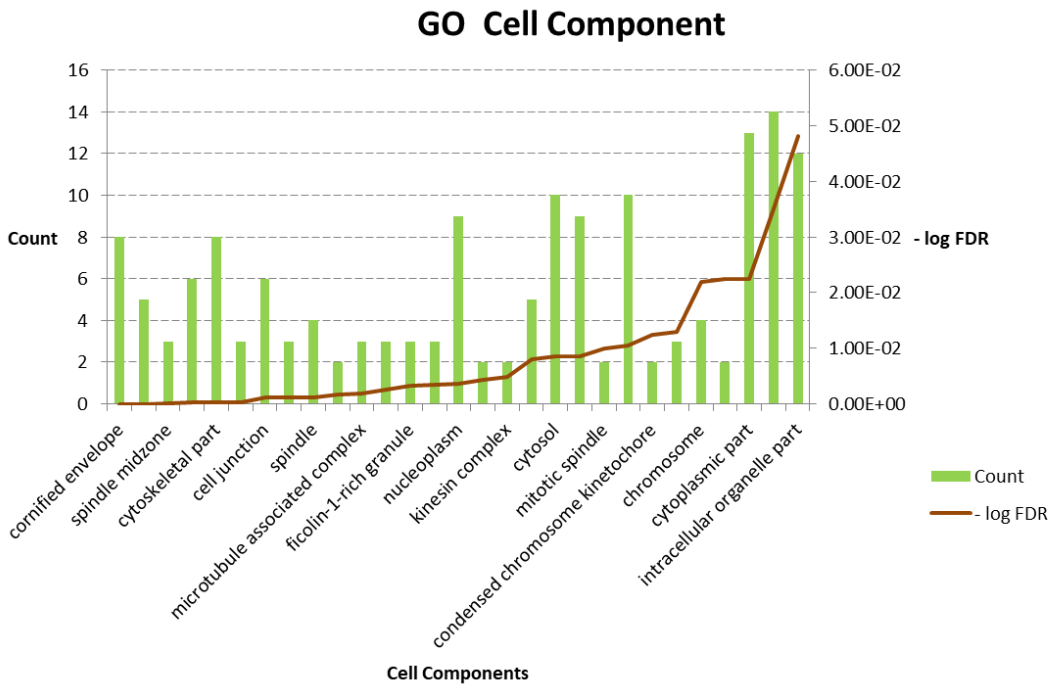
GO Cell Component
Count
- log FDR
Count
- log FDR
cornified envelope
spindle midzone
cytoskeletal part
cell junction
spindle
microtubule associated complex
ficolin-1-rich granule
nucleoplasm
kinesin complex
cytosol
mitotic spindle
condensed chromosome kinetochore
chromosome
cytoplasmic part
intracellular organelle part
Cell Components

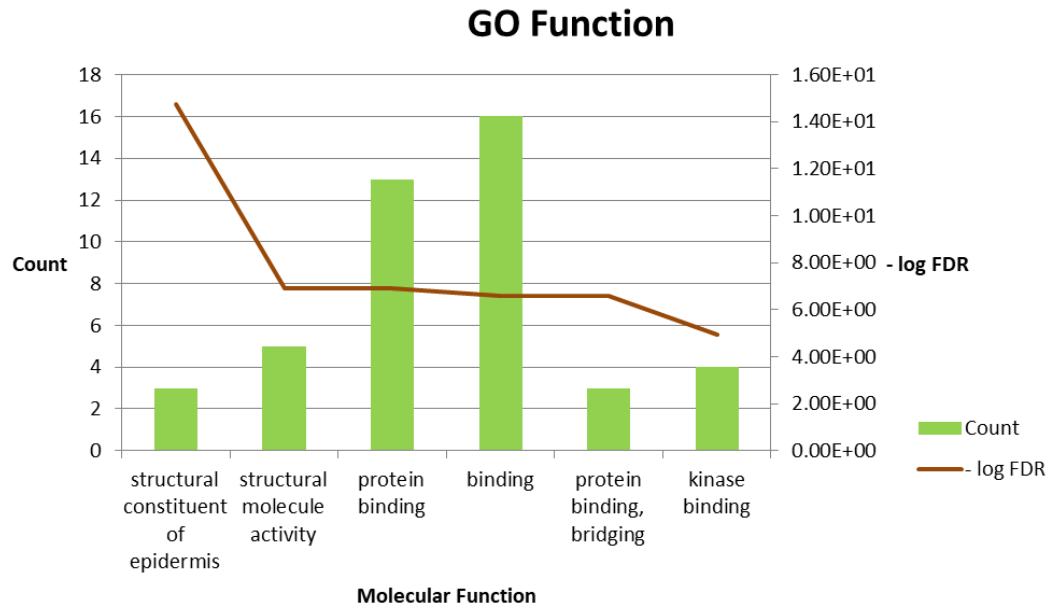
GO Function
Count
- log FDR
Count
- log FDR
structural constituent of epidermis
structural molecule activity
protein binding
binding
protein binding, bridging
kinase binding
Molecular Function

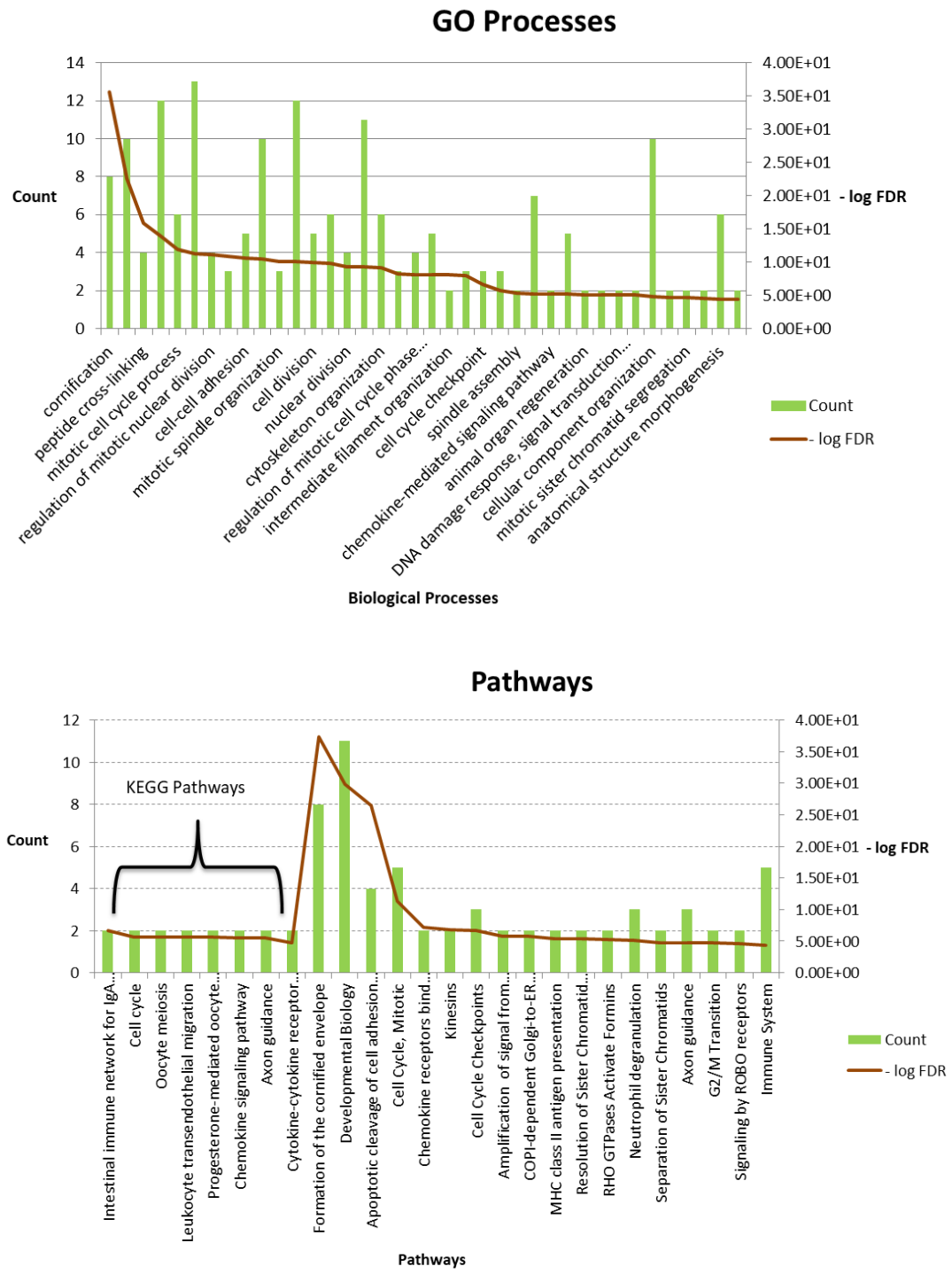

Figure 5.12 GO analysis and significantly enriched GO terms for Hub Genes in MCC. GO analysis classified the Hub Genes into three groups (molecular function, biological process, and cellular component). Significantly enriched KEGG pathways and Reactome pathways for Hub Genes in MCC.

Six hub genes, AURKA, BUB1, CDC6, CENPE, FOXM1 and KIF4A were found in Cluster A.

5.2 Identification of differentially expressed microRNAs in Merkel Cell Carcinoma

5.2.1 Identification and Selection of GEO datasets

A total of 5 data series from GEO were evaluated for Merkel Cell Carcinoma microRNA using keywords, 'Merkel Cell Carcinoma', 'Homo sapiens' and 'Non-coding RNA profiling by array'. 4 data series were excluded on the basis of treatment based studies, design of the study and other dataset details. Finally, 1 data series was found suitable for the purpose of this study and was downloaded from GEO, GSE45146. 2 samples of normal skin and 6 samples of MCC (including both primary and metastatic tumor samples) were chosen for this study.

5.2.2 Identification of differentially expressed microRNAs

The series GSE45146 was used to identify DEmiRNAs between normal skin samples and MCC. GEO2R (http://www.ncbi.nlm.nih.gov/geo/geo2r/), an online tool that performs comparisons on GEO datasets based on the GEOquery and Limma R packages, was used to identify DEmiRNAs. The miRNAs that met the cut-off criteria of the adjusted P-value (adj. P) <0.01 and |log fold change| >1.5 were considered to be DEmiRNAs. BH method was used for multiple test corrections. A total of 17 DEmiRNAs were identified which included 1 upregulated miRNA and 16 downregulated miRNAs.

ID	adj.P.Val	logFC
Downregulated		
hsa-miR-375	1.22E-05	-9.24833
hsa-miR-9*	1.22E-05	-8.70536
hsa-miR-9	1.71E-05	-8.24161
hsa-miR-18a	2.51E-05	-8.22654
hsa-miR-873	0.000039	-7.80773
hsa-miR-501-3p	0.000039	-7.69214
hsa-miR-454	4.95E-05	-7.43868
hsa-miR-195*	9.64E-05	-6.87839
hsa-miR-181c*	0.000225	-7.48504
hsa-miR-1	0.001778	-7.37286
hsa-miR-502-3p	0.007095	-2.71183
hsa-miR-518b	0.019113	-5.71209
hsa-miR-18b	0.020437	-6.64246
hsa-miR-590-5p	0.037281	-1.6829
hsa-miR-181c	0.037281	-5.40376
hsa-miR-19a	0.037281	-1.61635
Upregulated		
hsa-miR-221*	0.019009	7.402

Table 5.6 Differentially expressed microRNA (DEmiRNAs). Upregulated and downregulated microRNAs in MCC.

5.2.3 DEmicroRNA-Target Gene prediction

To identify putative target genes of the DEmiRs, three online resources were used. TargetScan Human version 7.2 (http://www.targetscan.org/vert_72/) and miRDB (http://mirdb.org/) were used to identify predictive miRNA-gene pairs while miRTarBase (http://mirtarbase.mbc.nctu.edu.tw/php/index.php) was used to identify experimentally validated miRNA-gene pairs. A total of 55,684 target interactions (experimental and predictive) were identified as putative targets for the 17 DEmiRs gathered in this study.

The data acquired was then used to identify validated and predictive pairs of DEGs-DEmiRs from this study. Out of a possible of 956 individual genes, 28 genes were found to be overlapping with the DEGs as well. These include ABHD5, CA12, CD164, CDH1, CLIP1, COLEC12, CXCR4, DEPDC1, EGLN3, ELAVL2, EREG, HIPK3, IGF1, IGF2BP3, KLF4, KLF5, MBNL1, MBNL2, NAB1, PICALM, RECK, RORA, SOX9, TM4SF1, TWF1, VAMP3, VSNL1 and WDR1.

56 pairs of validated DEGs-DEmiRs and 221 pairs of predicted DEGs-DEmiRs were curated from miRTarBase and TargetScan & miRDB respectively.

S.No	miRNA	Gene	S.No	miRNA	Gene	S.No	miRNA	Gene	S.No	miRNA	Gene
1	has-miR-454	ABHD5	56	has-miR-375	ELAVL2	111	has-miR-1	KLF4	166	hsa-miR-195-3p	RORA
2	has-mir-19a	ABHD5	57	hsa-miR-195-3p	ELAVL2	112	hsa-miR-18a	KLF5	167	hsa-mir-18b	RORA
3	has-mir-19a	ABHD5	58	has-mir-181c	ELAVL2	113	has-miR-375	KLF5	168	has-mir-181c	RORA
4	hsa-miR-181c-3p	ABHD5	59	hsa-miR-375	ELAVL2	114	hsa-miR-9-5p	KLF5	169	has-miR-1	RORA
5	has-mir-181c	ABHD5	60	hsa-miR-501-3p	ELAVL2	115	has-mir-590-5p	KLF5	170	hsa-miR-18a	RORA
6	has-miR-873	ABHD5	61	hsa-miR-502-3p	ELAVL2	116	hsa-miR-9-5p	KLF5	171	has-miR-873	RORA
7	has-miR-454	ABHD5	62	hsa-miR-221-3p	ELAVL2	117	hsa-miR-375	KLF5	172	hsa-miR-9-5p	RORA
8	hsa-miR-9-3p	ABHD5	63	hsa-miR-9-5p	ELAVL2	118	hsa-miR-18a	KLF5	173	hsa-miR-195-3p	RORA
9	has-miR-873	CA12	64	hsa-miR-195-3p	ELAVL2	119	hsa-miR-195-3p	KLF5	174	has-mir-19a	RORA
10	hsa-mir-18b	CA12	65	has-miR-1	ELAVL2	120	hsa-miR-9-3p	KLF5	175	has-miR-873	RORA
11	hsa-mir-18a	CA12	66	has-miR-454	EREG	121	hsa-miR-221-5p	MBNL1	176	has-miR-1	RORA
12	has-miR-1	CA12	67	has-mir-19a	EREG	122	has-miR-454	MBNL1	177	hsa-miR-9-5p	RORA
13	hsa-miR-181c-3p	CA12	68	has-miR-1	EREG	123	has-miR-375	MBNL1	178	has-miR-1	SOX9
14	has-mir-181c	CA12	69	has-miR-454	EREG	124	has-mir-590-5p	MBNL1	179	has-miR-1	SOX9
15	has-miR-873	CA12	70	has-mir-19a	EREG	125	hsa-miR-9-5p	MBNL1	180	hsa-miR-9-3p	SOX9
16	has-mir-181c	CA12	71	hsa-miR-195-3p	EREG	126	hsa-mir-18b	MBNL1	181	has-miR-1	TM4SF1
17	hsa-miR-18a	CA12	72	has-miR-1	EREG	127	hsa-miR-9-3p	MBNL1	182	hsa-miR-18a	TM4SF1
18	has-mir-19a	CD164	73	hsa-miR-9-3p	HIPK3	128	has-mir-181c	MBNL1	183	has-miR-1	TM4SF1
19	has-miR-1	CD164	74	has-mir-590-5p	HIPK3	129	hsa-miR-18a	MBNL1	184	has-mir-19a	TM4SF1
20	has-miR-1	CD164	75	has-mir-181c	HIPK3	130	has-mir-19a	MBNL1	185	has-miR-873	TM4SF1
21	has-mir-19a	CD164	76	has-miR-1	HIPK3	131	has-miR-454	MBNL1	186	has-miR-1	TWF1
22	hsa-miR-9-3p	CD164	77	hsa-miR-9-5p	HIPK3	132	has-mir-590-5p	MBNL1	187	hsa-mir-18b	TWF1
23	hsa-miR-9-3p	CDH1	78	has-mir-19a	HIPK3	133	hsa-miR-375	MBNL1	188	hsa-miR-18a	TWF1
24	hsa-miR-9-3p	CDH1	79	has-mir-590-5p	HIPK3	134	hsa-miR-195-3p	MBNL1	189	has-miR-1	TWF1
25	hsa-miR-9-5p	CDH1	80	has-mir-19a	HIPK3	135	hsa-miR-9-5p	MBNL1	190	hsa-miR-9-3p	TWF1
26	has-miR-873	CDH1	81	hsa-miR-221-3p	HIPK3	136	has-mir-19a	MBNL1	191	has-mir-19a	TWF1
27	hsa-miR-195-3p	CDH1	82	has-miR-1	HIPK3	137	hsa-miR-9-3p	MBNL1	192	hsa-miR-9-5p	VAMP3
28	has-miR-454	CLIP1	83	hsa-miR-195-3p	HIPK3	138	has-mir-19a	MBNL2	193	has-mir-19a	VAMP3
29	has-mir-181c	CLIP1	84	sa-miR-181c-3	HIPK3	139	hsa-miR-18a	MBNL2	194	has-mir-19a	VAMP3
30	has-mir-19a	CLIP1	85	has-mir-181c	HIPK3	140	has-mir-181c	MBNL2	195	hsa-miR-9-5p	VAMP3
31	has-miR-454	CLIP1	86	hsa-miR-9-5p	HIPK3	141	hsa-miR-195-3p	MBNL2	196	hsa-miR-195-3p	VAMP3
32	has-mir-19a	CLIP1	87	has-miR-454	HIPK3	142	has-mir-19a	MBNL2	197	has-mir-590-5p	VSNL1
33	hsa-miR-9-5p	COLEC12	88	hsa-miR-9-3p	HIPK3	143	hsa-miR-18a	MBNL2	198	hsa-miR-195-3p	VSNL1
34	hsa-miR-9-5p	COLEC12	89	hsa-mir-18b	HIPK3	144	hsa-miR-195-3p	MBNL2	199	hsa-miR-195-3p	VSNL1
35	has-miR-1	COLEC12	90	hsa-miR-18a	HIPK3	145	hsa-miR-195-3p	NAB1	200	hsa-miR-18a	VSNL1
36	hsa-miR-9-3p	COLEC12	91	has-miR-454	IGF1	146	has-miR-1	NAB1	201	has-miR-873	VSNL1
37	has-miR-1	CXCR4	92	hsa-miR-9-3p	IGF1	147	has-mir-181c	NAB1	202	has-mir-19a	VSNL1
38	hsa-miR-9-5p	CXCR4	93	has-miR-1	IGF1	148	hsa-miR-195-3p	NAB1	203	has-miR-1	VSNL1
39	has-miR-1	CXCR4	94	has-mir-19a	IGF1	149	has-miR-1	NAB1	204	hsa-mir-518b	WDR1
40	hsa-miR-9-5p	CXCR4	95	hsa-mir-18b	IGF1	150	has-miR-873	NAB1	205	hsa-miR-9-3p	WDR1
41	hsa-miR-195-3p	CXCR4	96	hsa-miR-18a	IGF1	151	hsa-miR-9-3p	NAB1	206	has-miR-1	WDR1
42	has-miR-454	DEPDC1	97	has-miR-454	IGF1	152	has-miR-1	PICALM	207	has-mir-19a	WDR1
43	has-miR-454	DEPDC1	98	has-miR-1	IGF1	153	hsa-miR-195-3p	PICALM	208	has-miR-1	WDR1
44	hsa-miR-9-3p	DEPDC1	99	hsa-miR-221-3p	IGF1	154	has-miR-1	PICALM	209	has-mir-19a	WDR1
45	has-mir-19a	DEPDC1	100	has-mir-19a	IGF1	155	hsa-mir-18b	PICALM	210	hsa-mir-518b	WDR1
46	has-miR-454	EGLN3	101	hsa-miR-9-3p	IGF1	156	hsa-miR-195-3p	PICALM	211	hsa-miR-9-3p	WDR1
47	hsa-miR-9-5p	EGLN3	102	hsa-miR-9-5p	IGF1	157	has-mir-590-5p	RECK			
48	has-miR-873	EGLN3	103	hsa-miR-9-3p	IGF2BP3	158	has-mir-181c	RECK			
49	has-miR-873	EGLN3	104	hsa-miR-9-5p	IGF2BP3	159	has-mir-590-5p	RECK			
50	has-miR-454	EGLN3	105	hsa-miR-9-5p	IGF2BP3	160	hsa-miR-221-3p	RECK			
51	hsa-miR-9-5p	EGLN3	106	hsa-miR-9-3p	IGF2BP3	161	has-miR-454	RECK			
52	hsa-miR-18a	EGLN3	107	has-miR-873	IGF2BP3	162	hsa-miR-195-3p	RECK			
53	has-miR-1	EGLN3	108	has-miR-375	KLF4	163	has-mir-19a	RORA			
54	hsa-miR-501-3p	ELAVL2	109	has-miR-1	KLF4	164	hsa-miR-501-3p	RORA			
55	hsa-miR-502-3p	ELAVL2	110	hsa-miR-375	KLF4	165	hsa-miR-502-3p	RORA			

Table 5.7 221 pairs of predicted DEGs-DEmiRs curated from TargetScan & miRDB

S.No	miRNA	Gene	S.No	miRNA	Gene
1	has-mir-19a	ABHD5	**30**	hsa-mir-18b	IGF1
2	hsa-miR-501-3p	CA12	**31**	hsa-miR-9-5p	IGF2BP3
3	hsa-miR-502-3p	CA12	**32**	hsa-miR-375	KLF4
4	hsa-miR-18a	CA12	**33**	hsa-miR-9-5p	KLF5
5	hsa-mir-18b	CA12	**34**	has-mir-590-5p	MBNL1
6	has-mir-19a	CD164	**35**	has-miR-454	MBNL1
7	hsa-miR-9-3p	CDH1	**36**	has-mir-19a	MBNL1
8	has-mir-19a	CDH1	**37**	has-mir-19a	MBNL2
9	has-miR-1	CDH1	**38**	has-miR-1	NAB1
10	has-miR-454	CLIP1	**39**	has-miR-1	PICALM
11	has-mir-19a	CLIP1	**40**	has-mir-590-5p	RECK
12	hsa-miR-9-5p	COLEC12	**41**	hsa-mir-18b	RORA
13	hsa-miR-9-3p	CXCR4	**42**	has-miR-873	RORA
14	hsa-miR-9-5p	CXCR4	**43**	has-mir-19a	RORA
15	has-miR-454	DEPDC1	**44**	hsa-miR-18a	RORA
16	has-mir-19a	DEPDC1	**45**	has-miR-1	SOX9
17	has-miR-873	EGLN3	**46**	hsa-miR-9-5p	TM4SF1
18	hsa-miR-18a	EGLN3	**47**	has-miR-1	TM4SF1
19	has-miR-454	EGLN3	**48**	hsa-mir-18b	TWF1
20	hsa-miR-501-3p	ELAVL2	**49**	has-miR-1	TWF1
21	hsa-miR-502-3p	ELAVL2	**50**	hsa-miR-18a	TWF1
22	hsa-miR-375	ELAVL2	**51**	has-mir-19a	VAMP3
23	has-miR-454	EREG	**52**	has-miR-873	VAMP3
24	has-mir-19a	EREG	**53**	hsa-miR-195-3p	VSNL1
25	hsa-miR-181c-3p	HIPK3	**54**	has-miR-873	VSNL1
26	has-mir-181c	HIPK3	**55**	hsa-miR-375	WDR1
27	has-mir-19a	HIPK3	**56**	has-mir-19a	WDR1
28	has-miR-1	HIPK3			
29	has-miR-1	IGF1			

Table 5.8 56 Validated pairs of DEGs-DEmiRs found using miRTarBase.

5.2.4 Construction and analysis of DEG-DEmiR network

The DEGs and DEmiRs were used to construct a dysregulation network using Cytoscape. The network consisted of 47 nodes and 267 edges.

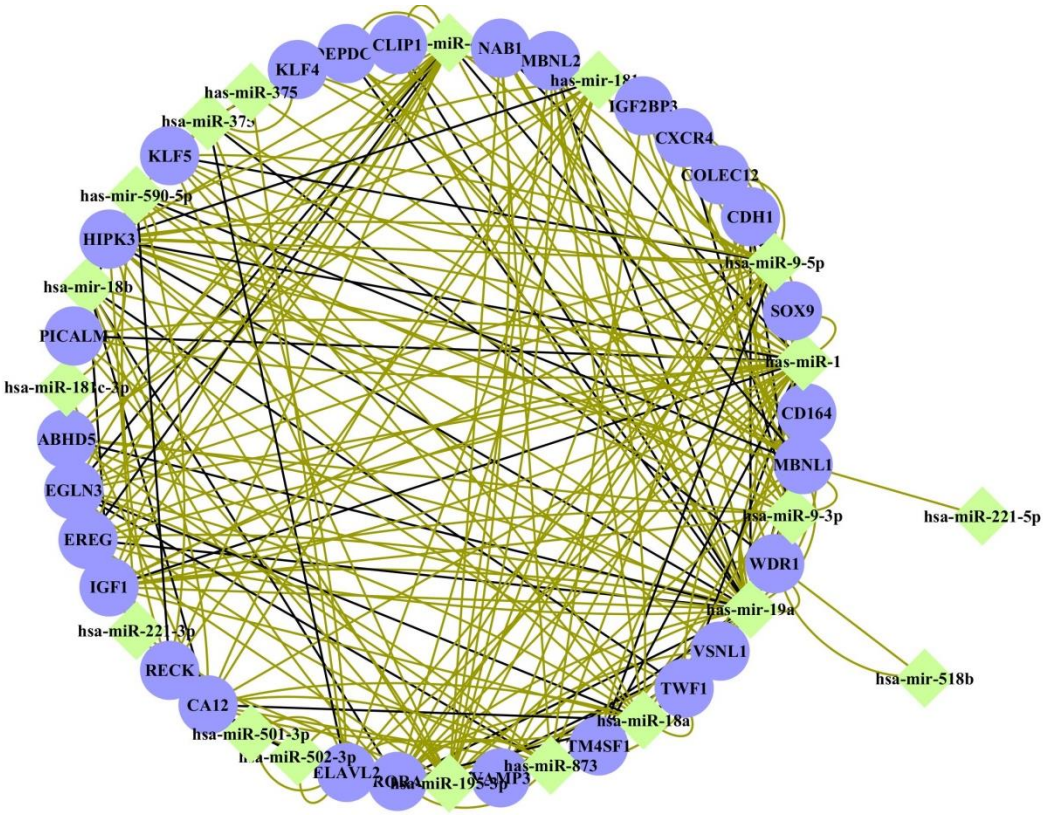

Figure 5.13 DEG-DEmiR network in Merkel Cell Carcinoma. In the circular layout, green and diamond shaped nodes represent DEmiRs and purple and circle nodes represent DEGs. The validated interactions are represented by black edge colour while the predictive interactions are represented by dark green edge colour.

Using Network Analyser tool of Cytoscape, the above network was analysed for the purpose of finding hub miRNAs. A degree cut-off of > 20 was set as the criteria, and the following miRNAs were shortlisted: hsa-miR-1, hsa-miR-19a, hsa-miR-9-5p, hsa-miR-9-3p, hsa-miR-454 and hsa-miR-195-3p. The three major hubs identified were hsa-miR-1, hsa-miR-19a and hsa-miR-9-5p.

Annotation of hub 'hsa-miR-1'

The hub "has-miR-1' was the major hub in the DEG-DEmiR network with a total of 39 degrees. These include CA12, CD164, CDH1, COLEC12, CXCR4, EGLN3, ELAVL2, EREG, HIPK3, IGF1, KLF4, NAB1, PICALM, RORA, SOX9, TM4SF1, TWF1, VSNL1 and WDR1. The annotation of this hub was carried out by DAVID, specifically for GO biological processes, GO molecular function and KEGG pathways. GO molecular function enriched were cadherin binding involved in cell-

cell adhesion, core promoter sequence-specific DNA binding and beta-catenin binding. In the GO biological processes group, positive regulation of transcription, DNA-templated, mRNA transcription, negative regulation of transcription, DNA-templated, positive regulation of transcription regulatory region DNA binding, ERK1 and ERK2 cascade, positive regulation of mitotic nuclear division, protein kinase B signalling and positive regulation of DNA replication were enriched. The primary pathway highlighted was 'pathways in cancer'.

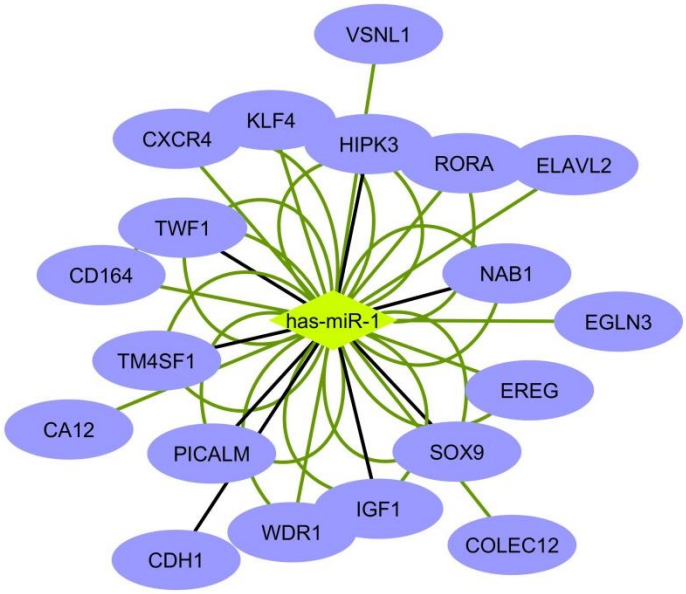

Figure 5.14 Subnetwork of DEG-DEmiR network with hub DEmiR, hsa-miR-1. The genes are represented by purple circular nodes. The dark green edges represent predictive pairing while black edges represent validated pairing. The network consists of 20 nodes and 39 edges.

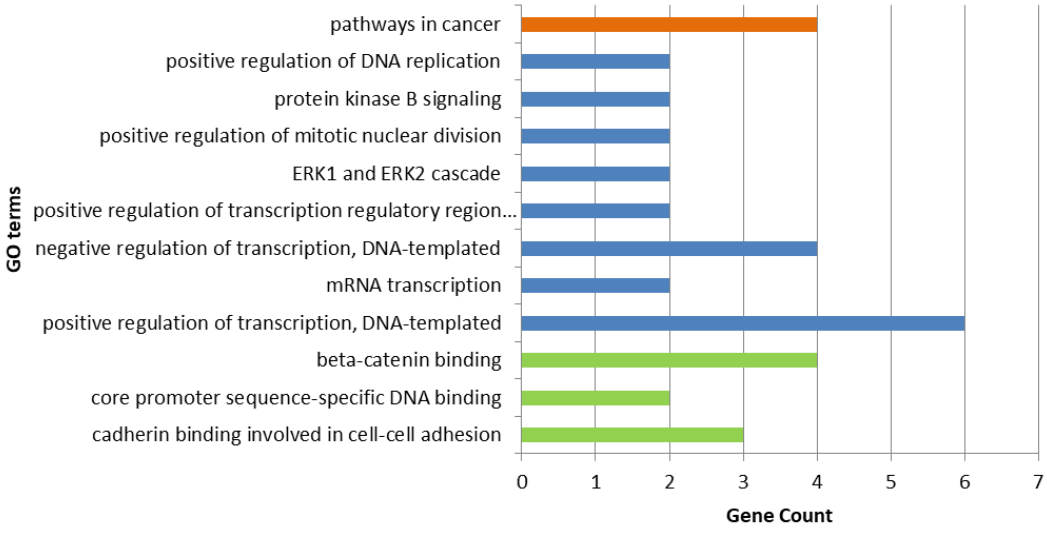

Molecular Function	Genes
cadherin binding involved in cell-cell adhesion	CDH1, PICALM, TWF1
core promoter sequence-specific DNA binding	RORA, SOX9
beta-catenin binding	RORA, CHD1, SOX9,KLF4
Biological Process	
positive regulation of transcription, DNA-templated	PICALM, IGF1, CDH1, RORA, SOX9, KLF4
mRNA transcription	EREG, HIPK3
negative regulation of transcription, DNA-templated	EREG, NAB1, SOX9, KLF4
positive regulation of transcription regulatory region DNA binding	IGF1, KLF4
ERK1 and ERK2 cascade	IGF1, SOX9
positive regulation of mitotic nuclear division	EREG, IGF1
protein kinase B signaling	IGF1, SOX9
positive regulation of DNA replication	EREG, IGF1
Pathways	
Pathways in Cancer	CXCR4, CDH1, EGLN3, IGF1

Figure 5.15 (a) Bar graph of GO terms enriched in hub 'hsa-miR-1'. Orange bar represents pathways, blue graphs represent biological processes and green bars represent molecular functions. All terms with p-value < 0.05 were considered statistically significant (b) Tabular representation of genes involved in the GO enriched terms

Annotation of hub 'hsa-miR-19a'

The second major hub in the network, with 38 degrees, was hsa-miR-19a. the 16 genes present in this module were as follows: ABHD5, CD164, CDH1, CLIP1, DEPDC1, EREG, HIPK3, IGF1, MBNL1, MBNL2, RORA, TM4SF1, TWF1, VAMP3, VSNL1 and WDR1.This hub was annotated in a couple of biological pathways, namely, mRNA transcription, myoblast differentiation, positive regulation of mitotic nuclear division, regulation of RNA splicing, positive regulation of DNA replication, positive regulation of fibroblast proliferation and positive regulation of smooth muscle cell proliferation. Only one pathway was highlighted, RHO GTPases activate IQGAPs with a fold enrichment score of 66.7 and a p-value of 0.026.

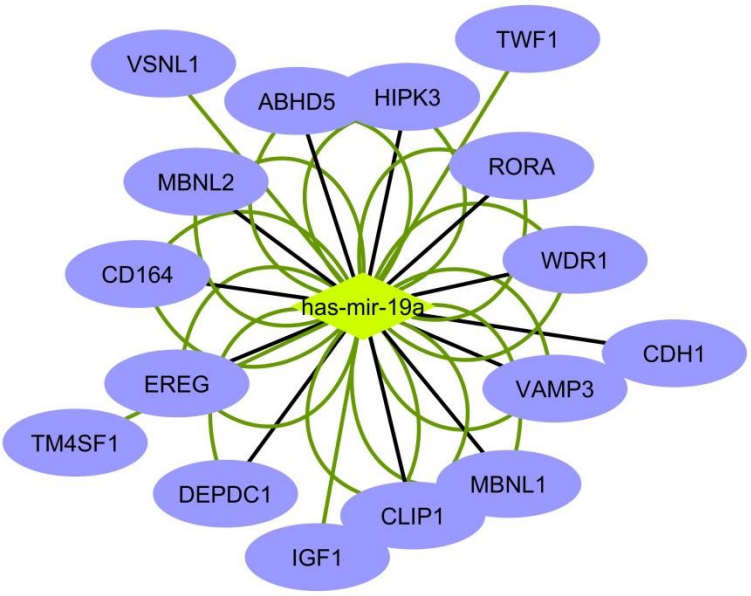

Figure 5.16 Subnetwork of DEG-DEmiR network with hub DEmiR, hsa-miR-19a. The genes are represented by purple circular nodes. The dark green edges represent predictive pairing while black edges represent validated pairing. The network consists of 17 nodes and 38 edges.

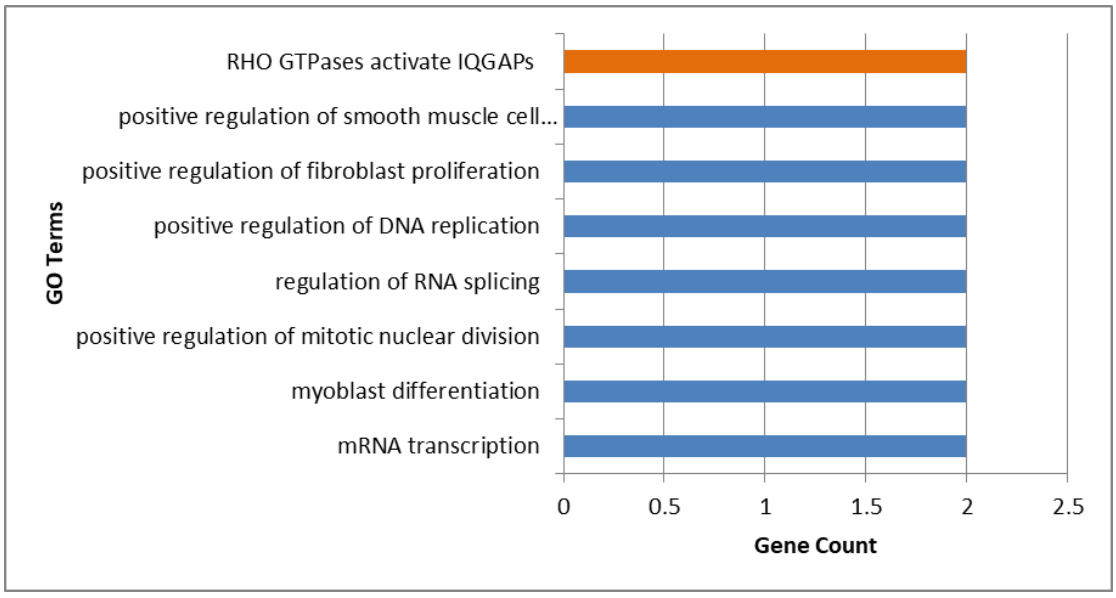

Biological Processes	Genes
mRNA transcription	EREG, HIPK3
myoblast differentiation	IGF1, MBNL1
positive regulation of mitotic nuclear division	EREG, IGF1
regulation of RNA splicing	MBNL2, MBNL1
positive regulation of DNA replication	EREG, IGF1
positive regulation of fibroblast proliferation	EREG, IGF1
positive regulation of smooth muscle cell proliferation	EREG, IGF1
Pathways	
RHO GTPases activate IQGAPs	CLIP1,CHD1

Figure 5.17 a) Bar graph of GO terms enriched in hub 'hsa-miR-19a'. Orange bar represents pathways and blue graphs represent biological processes. All terms with p-value < 0.05 were considered statistically significant (b) Tabular representation of genes involved in the GO nriched terms

Annotation of hub 'hsa-miR-9-5p'

This hub, with 26 degrees, was enriched with positive regulation of transcription, DNA-templated, myoblast differentiation and apoptotic process as biological processes. mRNA 3'-UTR binding, protein binding and RNA binding were the molecular functions highlighted. Only one pathway was identified, 'pathways in cancer' with a fold enrichment of 10.0 and a p-value of 0.0033. The genes involved in this module were CDH1, COLEC12, CXCR4, EGLN3, ELAVL2, HIPK3, IGF1, IGF2BP3, KLF5, MBNL1, RORA, TM4SF1 and VAMP3

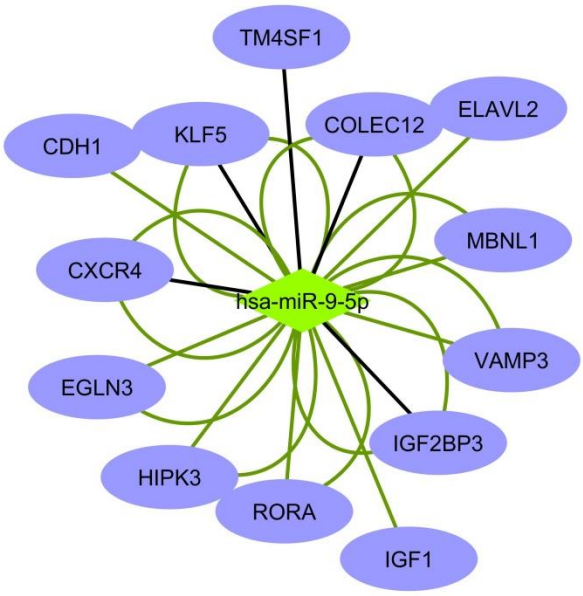

Figure 5.18 Subnetwork of DEG-DEmiR network with hub DEmiR, hsa-miR-9-5p. The genes are represented by purple circular nodes. The dark green edges represent predictive pairing while black edges represent validated pairing. The network consists of 14 nodes and 26 edges.

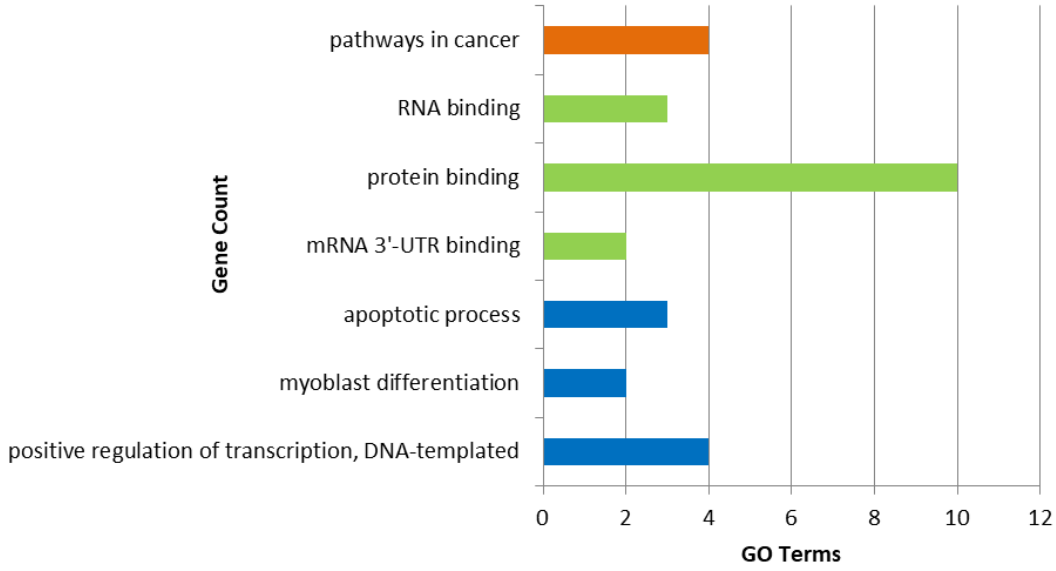

Biological processes	Genes
positive regulation of transcription, DNA-templated	RORA, CHD1, KLF5, IGF1
myoblast differentiation	MBNL1, IGF1
apoptotic process	CXCR4, EGLN3, HIPK3
Molecular functions	
mRNA 3'-UTR binding	ELAVL2, IGF2BP3
protein binding	MBNL1,ELAVL2, IGF2BP3, CX
RNA binding	MBNL1,ELAVL2, IGF2BP3
Pathways	
pathways in cancer	CXCR4, CDH1, EGLN3, IGF1

Figure 5.19 (a) Bar graph of GO terms enriched in hub 'hsa-miR-9-5p'. Orange bar represents pathways, blue graphs represent biological processes and green bars represent molecular functions. All terms with p-value < 0.05 were considered statistically significant (b) Tabular representation of genes involved in the GO enriched terms.

PART VI
DISCUSSION

6 DISCUSSION

Merkel Cell Carcinoma (MCC) is an aggressive form of neuroendocrine carcinoma. It represents the 2nd highest cause of skin cancer related deaths despite being a relatively rare form of cancer (Schadendorf et al, 2017). Different risk factors have been associated with MCC such as advancement age, immunosuppression, and ultraviolet light exposure, polyomavirus infection and a current, concurrent or previous diagnosis of Chronic Lymphocytic Leukaemia (CLL) (Kaae et al, 2010). However, the exact mechanism that leads to MCC and its inherent biology is yet to be fully researched and explored. The current treatments for MCC are a combination of surgery and radiation or chemo-radiation. So far, only two drugs have been approved by FDA for the treatment of MCC, with both drugs being immune checkpoint inhibitors. However, the drug approval from FDA was accelerated based on promising results from a relatively small number of patients, which means that the more research and trials are undergoing currently considering the fact that a very small cohort was used for clinical trials. Although, 56% of the drug recipients have shown a positive response, many stopped using the drug due to severe side effects. A further issue is that many patients with MCC may not be ideal candidates for immunotherapy because their immune systems have been suppressed—due to organ/graft transplantation, lymphoma or HIV (Nghiem et al, 2016).

Presently there are no biomarkers indicative of MCC and additional research is essential. With the advent of bioinformatics and microarray technology, in silico approaches pertaining to 'omics' data analysis may shed light on hub genes and miRNAs for clinical utility.

In this study, one dataset was identified for comparing the differences in mRNA expression in normal skin samples and MCC samples. Eventually, a total of 449 DEGs were screened including 164 upregulated and 285 downregulated genes. Functional analysis revealed significant enrichment in positive regulation of transcription from RNA polymerase II promoter, positive regulation of cell proliferation, oxidation-reduction process, epidermis development in the BP group. IN CC, cytoplasm, plasma membrane, extracellular exosome, extracellular region

and integral component of plasma membrane were highlighted. Protein binding, calcium ion binding, protein homo-dimerization activity, structural molecule activity and structural constituent of cytoskeleton were the enriched MF terms. Additionally, pathways that were enriched included cAMP signaling pathway, calcium signaling pathway, arachidonic acid metabolism, inflammatory mediator regulation of TRP channels, p53 signaling pathway, aldosterone synthesis and secretion and GnRH signaling pathway.

Given the important role of Ca2+ signalling in various cellular processes (Clapham, 2007) it is not surprising that the Ca2+ signal is implicated in regulation of MCC-associated processes and pathways. In the context of cancer, important oncogenic machinery is often sensitive to regulation by definite Ca2+ signals (Monteith et al, 2012). Variations in the expression of specific Ca2+ channels and pumps have been commonly reported in quite a few types of cancer, for instance, increased ORAI1 channel expression have been found promoting Ca2+ proliferative pathways in oesophageal squamous cell carcinoma cells (Zhu, H. et al, 2014). Moreover, voltage-gated Ca2+ channels have also been linked to neuroendocrine-induced differentiation and proliferation (Mariot et al, 2002) an important indication given that MCC tumors are neuroendocrine in nature.

The arachidonic acid (AA) metabolism pathway has been implicated in diverse human cancers (Wang et al, 2010). Tumorigenesis is promoted by genotoxic agents such as peroxides and reactive oxygen species that are produced by this pathway (Gorrini et al, 2013). AAM pathway reportedly promotes tumor progression by activating major pathways, including PI3K and MAPK (Hughes-Fulford et al, 2006; Paine et al, 2000). Previous studies by Hafner et al have confirmed that the activation of PI3K/AKT pathway in MCC and identifies PI3K/AKT as a potential new therapeutic target for MCC patients. Moreover, 7 DEGs were implicated in AAM pathway including AKR1C3, PLA2G4A, PTGIS, ALOX15B, PLA2G2A, EPHX2 and ALOX12B. Gene AKR1C3 has been shown to be overexpressed in skin SCC, another type of skin cancer (Mantel et al, 2014). In malignant melanoma cell lines, suggest an overexpression of PLA2 (Scuderi et al, 2008).

Overexpression and activation of other pathways is a known detail about genes of the AAM pathway (Marks et al, 2007). Taking into account the intensive studies of targets on this pathway in other diseases such as cardiovascular disease, an opportunity for drug repurposing of drugs already in clinical development arises (Hyde et al, 2009). Also, in accordance with previous studies, is the implication of p53 family member, p56, to be involved in poor prognosis in MCC (Asioli et al, 2007). Hence, targets on these pathways might be potentially novel therapy candidates.

The PPI network of DEGs was constructed with 448 nodes (including 38 isolated nodes) and 2190 edges. Subsequent significant module selection using MCODE highlighted three major clusters. In cluster A all 29 genes were upregulated, in cluster B all the 15 genes were downregulated while in cluster C 6 genes were upregulated and 6 genes were downregulated. A BP, MF, CC and pathway analysis of Cluster A showed that it was primarily enriched in cell cycle, cell cycle checkpoints, mitotic metaphase and anaphase, regulation of cell cycle and chromosome organisation. All of the abovementioned processes and pathways are often disordered or aberrant in human cancers. A previous study by Demetriou et al showed that an MCC cell line infected with MCV is suggestively impaired in its ability to respond to UVR-induced DNA damage comparative to a distinct uninfected MCC cell line. T antigen expression by MCV indeed inhibits key responses to UVR-induced DNA damage and suggests that progressive MCV-mediated retraction of genomic stability may be involved in Merkel cell carcinogenesis (Demetriou et al, 2012). Since 80% of MCC tumors are MCV positive, this is a significant result pertinent to MCC occurrence and progression. Cluster B analysis revealed enrichment in structural constituent of epidermis, cornified envelope, cell-cell adhesion and immune system. All of the above indications are in accordance with previous studies. The expression of Notch-1 and alteration of the E-cadherin/β-catenin cell adhesion complex were observed in merkel cell carcinoma. The downregulation of E-cadherin and diffuse membranous β-catenin expression suggested a dysregulation of the E-cadherin/β-catenin complex which may be involved in local invasion and distant metastasis (Panelos et al, 2019). The link of MCC with immune system has been greatly explored and hence the enrichment of this GO term was unsurprising. Patients with AIDS and solid organ transplant

recipients have an incidence rate of developing MCC greater than the general population (JC Becker, 2012). Moreover, numerous reports have described regression after an improvement in immune function, emphasizing the prominence of the immune system to the development of MCC (Wooff et al, 2010; Burack et al, 2003).

cytoHubba plugin was used to identify hub genes in the PPI network by observing an intersection of five algorithms (degree, MCC, MNC, EPC and EcCentricity). These include 16 genes: AURKA, FLG, KIF4A, DSG1, PKP1, LOR, BUB1, CDC6, CENPE, CXCR4, FOXM1, CXCL12, CDSN, DSG3, IVL and DSP. The 16 hubs genes included 7 upregulated and 9 downregulated genes and a network of these 16 hub genes revealed that the upregulated and downregulated genes were part of two individual clusters. An enrichment analysis showed that these genes were mostly enriched in cornified envelope, cytosol, programmed cell death, cornification, cell cycle, immune system and chemokine signalling pathway. The involvement and implication of all these GO terms have already been discussed, barring cornification and chemokine signalling pathway. While a relationship between cornification and MCC hasn't been reported in literature, it is an important aspect of terminal differentiation and programmed cell death in epidermal keratinocytes. Identifying the mechanisms governing cornification may help in directing non-differentiating cancerous keratinocytes towards cornification and their eventual cell death. Similarly, a relation between chemokine signalling and MCC has yet not been reported however, chemokine receptor, $CXCR_3$ and its ligands reportedly play a role in skin cancers (Kuo et al, 2018)

AURKA codes for a protein that appears to be a cell cycle-regulated kinase that is present in microtubule formation and/or stabilization at the spindle pole during chromosome segregation. AURKA is reportedly involved in tumor progression and has been studied in the context of skin cancers previously. Torchia et al, strongly suggested the Aurora-A overexpression in the malignant progression of skin tumors. AURKA overexpression is associated with poor prognosis in three independent cohorts of melanoma patients were shown by Puig-Butille et al. Another study showed the miR-137 aided tumor suppression in malignant melanoma cells by targeting of AURKA oncogene (Chang et al, 2016).

According to Human Protein Atlas (HPA), genes FLG, DSG1, LOR, CDSN and IVL show aberrant expression in skin cancers in comparison to normal skin samples. As per previous studies on MCC, genes DSG1, CXCR4 and CXCL12 have been reportedly linked to MCC. Brennen et al confirmed DSG2 as a potential marker for a variety of skin-derived carcinomas (BCC and SCC). Four distinct desmoglein genes (DSG1, DSG2, DSG3, and DSG4) have been implicated in cell-cell adhesion but their individual roles in carcinogenesis are poorly understood. Since genes DSG1 and DSG3 were identified as hub genes along with cell-cell adhesion and desmosomes as enriched GO terms, these genes might have important implications in tumorigenesis of MCC. In a study carried out by Knapp et al, although the role of CXCR4 in the progression of MCC was not fully clarified, their differential expression in more advanced stages of MCC might suggest an independence from more classic antiapoptotic and cell localization pathways. The homeostatic chemokine CXCL12 was expressed outside malignant nodules while its receptor CXCR4 was identified within MCC tumor (Wheat et al, 2014). The rest of the genes identified in this study haven't been reported previously in relation to MCC studies.

Further, dataset GSE45146 was selected and analysed for the purpose of identifying DEmiRs in MCC. A total of 17 DEmiRNAs were identified which included 1 upregulated miRNA and 16 downregulated miRNAs. A total of 55,684 target interactions (experimental and predictive) were identified as putative targets for the 17 DEmiRs gathered in this study. Out of a possible of 956 individual genes, 28 genes were found to be overlapping with the DEGs as well. 56 pairs of validated DEGs-DEmiRs and 221 pairs of predicted DEGs-DEmiRs were curated from miRTarBase and TargetScan & miRDB respectively. The DEGs and DEmiRs were used to construct a dysregulation network using Cytoscape. Using Network Analyser tool of Cytoscape the following miRNAs were shortlisted: *hsa-miR-1, hsa-miR-19a, hsa-miR-9-5p, hsa-miR-9-3p, hsa-miR-454* and *hsa-miR-195-3p*. The three major hubs identified were *hsa-miR-1, hsa-miR-19a* and *hsa-miR-9-5p.*

miRNAs are crucial components of cells in both normal and diseased conditions. The miRNA expression pattern of normal cells compared to pathogenic cells differs and as a result exosomal miRNAs are used as biomarkers for different malignancies, such as melanoma, breast, prostate and gastric cancer (Huang et al, 2015 ; Pfeffer et al, 2015 ; Imamura et al, 2017; Zhao et al, 2016). Due to the rarity of merkel cells, a

pattern of normal merkel cell miRNA expression has not yet been determined. This leads to a drawback in using MCC-derived miRNA as biomarkers. Hence, whether the expression of MCC-derived miRNAs is specific for normal cells or also shown by non-malignant cells, is still unknown. An additional problem is the lack of common miRNAs among the MCC expressed miRNAs identified so far. So far, miR-30a, miR-34 and miR-375 have been reported by Renwick et al and Xie et al. Another principle for a valuable biomarker is that it can predict the consequence of the disease. Further studies by Xie et al. revealed a link between higher levels of miR-150 with a poorer prognosis of MCC. Finally, miRNAs may also help in resolving the mystery surrounding the origin of Merkel cells. miRNA signatures may provide a different route than conventional immunhistochemical staining. That would requires the identification of cells that have been suggested to be the origin of Merkel cells such neural crest cells, keratinocytes, epidermal fibroblasts, early B cells and hair follicle stem cells. *hsa-miR-1* downregulation has been identified in lung (Melkamu et al, 2010), head and neck (Sarver et al, 2009), colon (Childs et al,2009) and hepatocellular cancer (Datta et al, 2008).

PART VII
CONCLUSION

7 CONCLUSION

MCC is an aggressive form of neuroendocrine carcinoma that represents the second most common cause of skin cancer related deaths. MCC is often associated with a poor prognosis, as more than one-third of patients die from the disease compared to ~15% for malignant melanoma. Due to the rarity of the disease and of the occurrence of merkel cells, MCC remains a cancer type that is yet to be fully researched and understood. This is of immediate consequence now as the incidences of MCC have been on a rise and the disease is often associated with fatality. In fact, only two FDA approved drugs exist in the market for treatment of MCC. Further, there are no biomarkers predictive of response that could help to better select patients to these new therapies, and additional research is essential. The current study identified hub genes and hub miRNAs associated with MCC using integrated bioinformatics along with their functional analysis, PPI network construction, module selection and module enrichment analyses. In conclusion, the findings of the current study may provide prerequisite for future studies to identify useful markers and understand underlying mechanisms related to MCC carcinogenesis. However, further research is required to validate the potential of the identified hub genes and hub miRNAs.

PART VIII
REFERENCES

8 REFERENCES

- Agelli M, Clegg LX. (2003). Epidemiology of primary Merkel cell carcinoma in the United States. *J Am Acad Dermatol*, *49*(5), 832–41.
- Amaral T, Leiter U, Garbe C. (2017). Merkel cell carcinoma: Epidemiology, pathogenesis, diagnosis and therapy. *Rev Endocr Metab Disord*, *18*(4), 517-532. doi: 10.1007/s11154-017-9433-0.
- Andea AA, Patel R, Ponnazhagan S, Kumar S, DeVilliers P, Jhala D, et al. (2010). Merkel cell carcinoma: correlation of KIT expression with survival and evaluation of KIT gene mutational status. *Hum Pathol, 41* (10), 1405-1412.
- Asioli S, Righi A, Volante M, et al. (2007). p63 expression as a new prognostic marker in Merkel cell carcinoma. *Cancer*, *110*(3), 640–7.
- BAVENCIO® (avelumab) https://www.accessdatafdagov/drugsatfda_docs/label/2017/761049s000lblpdf
- Becker JC. Merkel cell carcinoma. (2010). *Ann Oncol*, *21*(7), 81–85.
- Bichakjian CK, Lowe L, Lao CD, Sandler HM, Bradford CR, Johnson TM, et al. (2007). Merkel cell carcinoma: critical review with guidelines for multidisciplinary management. *Cancer*, *110* (1), 1-12.
- Brennan D & Mahoney MG. (2009). Increased expression of Dsg2 in malignant skin carcinomas: A tissue-microarray based study. *Cell adhesion & migration*, *3*(2), 148–154. doi:10.4161/cam.3.2.7539.
- Brunner M, Thurnher D, Pammer J, Heiduschka G, Petzelbauer P, Schmid C, et al. (2010). Expression of hedgehog signaling molecules in Merkel cell carcinoma. *Head Neck, 32* (3), 333-340.
- Burack J, Altschuler EL. (2003). Sustained remission of metastatic Merkel cell carcinoma with treatment of HIV infection. *J R Soc Med*. *9*(6), 238–239. doi: 10.1258/jrsm.96.5.238.
- Chang X, Zhang H, Lian S, Zhu W. (2016). MiR-137 suppresses tumor growth of malignant melanoma by targeting aurora kinase A. *Biochem Biophys Res Commun*, *475*(3), 251-6.

- Childs G, Fazzari M, Kung G et al. (2009). Low-level expression of microRNAs let-7d and miR-205 is prognostic markers of head and neck squamous cell carcinoma. *The American Journal of Pathology*, *174*(3), 736–745.
- Chou CH, Shrestha S, Yang CD, Chang NW, Lin YL, Liao KW, Huang WC, Sun TH, Tu SJ, Lee WH, Chiew MY, Tai CS, Wei TY, Tsai TR, Huang HT, Wang CY, Wu HY, Ho SY,Chen PR, Chuang CH, Hsieh PJ, Wu YS, Chen WL, Li MJ, Wu YC, Huang XY, Ng FL, Buddhakosai W, Huang PC, Lan KC, Huang CY, Weng SL, Cheng YN, Liang C, Hsu WL,Huang HD. (2018). miRTarBase update 2018: a resource for experimentally validated microRNA-target interactions. *Nucleic Acids Res*. *4(*46), 296-302.
- Cimino PJ, Robirds DH, Tripp SR, Pfeifer JD, Abel HJ, Duncavage EJ. (2014). Retinoblastoma gene mutations detected by whole exome sequencing of Merkel cell carcinoma. *Modern Pathol Off J United States Canad Acad Pathol Inc*, *27*(8), 1073–87.
- Clapham, D. E. (2007). Calcium signaling. *Cell*, 131, 1047–1058.
- Clarke CA, Robbins HA, Tatalovich Z, Lynch CF, Pawlish KS, Finch JL, et al. (2015). Risk of merkel cell carcinoma after solid organ transplantation. *J Natl Cancer Inst*., *107*(2).
- Cui XL. & Douglas JG. (1997). Arachidonic acid activates c-jun N-terminal kinase through NADPH oxidase in rabbit proximal tubular epithelial cells. *Proc. Natl Acad. Sci*, 94, 3771–3776.
- Dabner M, McClure RJ, Harvey NT, Budgeon CA, Beer TW, Amanuel B, et al. (2014). Merkel cell polyomavirus and p63 status in Merkel cell carcinoma by immunohistochemistry: Merkel cell polyomavirus positivity is inversely correlated with sun damage, but neither is correlated with outcome. *Pathology*, *46*(3), 205–10.
- Datta J, Kutay H, Nasser MW et al. (2008). Methylation mediated silencing of microRNA-1 gene and its role in hepatocellular carcinogenesis. *Cancer Research*, *68*(13), 5049–5058.
- Demetriou S K, Ona-Vu K, Sullivan EM, Dong TK, Hsu SW, & Oh DH. (2012). Defective DNA repair and cell cycle arrest in cells expressing Merkel cell polyomavirus T antigen. *International journal of cancer*, *131*(8), 1818–

1827.

- Engels EA, Frisch M, Goedert JJ, Biggar RJ, Miller RW. (2002). Merkel cell carcinoma and HIV infection. *Lancet*, *359*(9305), 497–8.
- Erstad DJ, Jr JC. (2014). Mutational analysis of merkel cell carcinoma. *Cancer*, 6(4), 2116–36.
- Feng H, Kwun HJ, Liu X, Gjoerup O, Stolz DB, Chang Y, et al. (2011). Cellular and viral factors regulating Merkel cell polyomavirus replication. *PLoS One*, *6*(7).
- Fernandez-Figueras MT, Puig L, Musulen E, et al. (2007). Expression profiles associated with aggressive behaviour in Merkel cell carcinoma. *Mod Pathol*, *20*(1), 90–101.
- Fernandez-Figueras MT, Puig L, Musulen E, Gilaberte M, Ferrandiz C, Lerma E, et al. (2005). Prognostic significance of p27Kip1, p45Skp2 and Ki67 expression profiles in Merkel cell carcinoma, extra cutaneous small cell carcinoma, and cutaneous squamous cell carcinoma. *Histopathology*, *46* (6), 614-621.
- Fitzgerald TL, Dennis S, Kachare SD, et al. (2015). Dramatic increase in the incidence and mortality from Merkel cell carcinoma in the United States. *Am Surg*, 81(8), 802–6.
- Girschik J, Thorn K, Beer TW, Heenan PJ, Fritschi L. (2011). Merkel cell carcinoma in Western Australia: A population-based study of incidence and survival. *Br J Dermatol*, *165*(5), 1051–7.
- Goh G, Walradt T, Markarov V, Blom A, Riaz N, Doumani R, et al. (2016). Mutational landscape of MCPyV-positive and MCPyV negative Merkel cell carcinomas with implications for immunotherapy. *Oncotarget*, *7*(3), 3403–15.
- Gonzalez-Vela MD, Curiel-Olmo S, Derdak S, Beltran S, Santibanez M, Martinez N, et al. (2017). Shared oncogenic pathways implicated in both virus-positive and UV-induced Merkel cell carcinomas. *J Invest Dermatol*, *137*(1), 197–206.
- Gorrini, C., Harris, IS. & Mak, TW. (2013). Modulation of oxidative stress as an anticancer strategy. *Nat. Rev. Drug Discov*. *12*(12), 931–947.
- Gu J, Polak JM, VanNoorden S, Pearse AG, Marangos PJ, Azzopardi JG.

(1983). Immunostaining of neuron-specific enolase as a diagnostic tool for Merkel cell tumors *Cancer, 52* (6), 1039-1043.

- Hafner C, Houben R, Baeurle A, Ritter C, Schrama D, Landthaler M, et al. (2012) Activation of the PI3K/AKT Pathway in Merkel Cell Carcinoma. *PLoS ONE 7(*2).
- Han W, Soltani K, Ming M, He YY. (2012). Deregulation of XPC and CypA by cyclosporin a: An immunosuppression-independent mechanism of skin carcinogenesis. *Cancer Prev Res, 5*(9), 1155–62.
- Hanly AJ, Elgart GW, Jorda M, Smith J, Nadji M. (2000). Analysis of thyroid transcription factor-1 and cytokeratin 20 separates Merkel cell carcinoma from small cell carcinoma of lung. *J Cutan Pathol*, *27* (3), 118-120.
- Harms PW, Vats P, Verhaegen ME, Robinson DR, Wu YM, Dhanasekaran SM, et al. (2015). The distinctive mutational spectra of polyomavirus-negative Merkel cell carcinoma. *Cancer Res*, *75*(18), 3720–7.
- Harms PW. (2017). Update on Merkel Cell Carcinoma. *Clin Lab Med*, *37*(3), 485-501.
- Heath M, Jaimes N, Lemos B, Mostaghimi A, Wang LC, Penas PF, et al. (2008). Clinical characteristics of Merkel cell carcinoma at diagnosis in 195 patients: the AEIOU features. *J Am Acad Dermatol*, *58* (3), 375-381.
- Howard RA, Dores GM, Curtis RE, Anderson WF, Travis LB. (2006). Merkel cell carcinoma and multiple primary cancers. *Cancer Epidemiol Biomark Prev*, *15*(8), 1545–9.
- Huang X, Yuan T, Liang M, Du M, Xia S, Dittmar R, Wang D, See W, Costello BA, Quevedo F, Tan W, Nandy D, Bevan GH, Longenbach S, Sun Z, Lu Y,Wang T, Thibodeau SN, Boardman L, Kohli M, Wang L. (2014). Exosomal miR-1290 and miR-375 as prognostic markers in castration-resistant prostate cancer. *Eur Urol*, *67*(1), 3-41.
- Hughes-Fulford M, Li CF, Boonyaratanakornkit J. & Sayyah S. (2006). Arachidonic acid activates phosphatidylinositol 3-kinase signaling and induces gene expression in prostate cancer. *Cancer Res*, *66*(3), 1427–1433.
- Hyde CA & Missailidis S. (2009). Inhibition of arachidonic acid metabolism and its implication on cell proliferation and tumour-angiogenesis. *Int. Immunopharmacol*, *9*(6), 701–715.

- Imamura T, Komatsu S, Ichikawa D, Miyamae M, Okajima W, Ohashi T, Kiuchi J, Nishibeppu K, Kosuga T, Konishi H, Shiozaki A, Okamoto K, Fujiwara H, Otsuji E.(2017). Low plasma levels of miR-101 are associated with tumor progression in gastric cancer. *Oncotarget*, *8*(63), 106538-106550.
- Jaeger T, Ring J, Andres C. (2012). Histological, immunohistological, and clinical features of Merkel cell carcinoma in correlation to Merkel cell polyomavirus status. *J Skin Cancer*. doi: 10.1155/2012/983421.
- Kaae J, Hansen AV, Biggar RJ, Boyd HA, Moore PS, Wohlfahrt J, et al. (2010). Merkel cell carcinoma: incidence, mortality, and risk of other cancers. *J Natl Cancer Inst*, *102* (11), 793-801.
- Kaufman HL, Russell J, Hamid O, Bhatia S, Terheyden P, D'Angelo SP, et al. (2016). Avelumab in patients with chemotherapy refractory metastatic Merkel cell carcinoma: A multicentre, single-group, open-label, phase 2 trial. *Lancet Oncol*, *17*(10), 1374–85.
- Kempf W, Mertz KD, Hofbauer GF, Tinguely M. (2013). Skin cancer in organ transplant recipients. *Pathobiol J Immunopathol Mol Cellr Biol*, *80*(6), 302–9.
- Koksal Y, Toy H, Talim B, Unal E, Akcoren Z, Cengiz M. (2009). Merkel cell carcinoma in a child. *J Pediatr Hematol Oncol*, *31*(5), 359–61.
- Kuo PT, Zeng Z, Salim N, Mattarollo S, Wells JW, Leggatt GR. (2018). The Role of CXCR3 and Its Chemokine Ligands in Skin Disease and Cancer. *Front Med (Lausanne)*. doi: 10.3389/fmed.2018.00271.
- Kurzen H, Kaul S, Egner U, Deichmann M, Hartschuh W. (2003). Expression of MUC 1 and ep-CAM in Merkel cell carcinomas: implications for immunotherapy. *Arch Dermatol Res*, *295* (4), 146-154.
- Lanoy E, Costagliola D, Engels EA. (2010). Skin cancers associated with HIV infection and solid-organ transplantation among elderly adults. *Int J Cancer*, *126*(7), 1724–31.
- Lebbe JC, Becker JJ, Grob J, Malvehy V Del Marmol, Pehamberger H, et al.(2015). Diagnosis and treatment of Merkel cell carcinoma. European consensus-based interdisciplinary guideline. *Eur J Cancer*, *51* (16), 2396-2403.

- Lemos BD, Storer BE, Iyer JG, Phillips JL, Bichakjian CK, Fang LC, et al. (2010). Pathologic nodal evaluation improves prognostic accuracy in Merkel cell carcinoma: analysis of 5823 cases as the basis of the first consensus staging system. *J Am Acad Dermatol*, *63* (5), 751-761.
- Leroux-Kozal V, Leveque N, Brodard V, Lesage C, Dudez O, Makeieff M, et al. (2015). Merkel cell carcinoma: Histopathologic and prognostic features according to the immunohistochemical expression of Merkel cell polyomavirus large T antigen correlated with viral load. *Hum Pathol*, *46*(3), 443–53.
- Lewis BP, Burge CB, Bartel DP. (2005). Conserved seed pairing, often flanked by adenosines, indicates that thousands of human genes are microRNA targets. *Cell*, *120*(1), 15-20.
- Lipson EJ, Vincent JG, Loyo M, et al. (2013). PD-L1 expression in the Merkel cell carcinoma microenvironment: association with inflammation, Merkel cell polyomavirus and overall survival. *Cancer Immunol Res*, *1(*1), 54–63.
- Lipson EJ, Vincent JG, Loyo M, Kagohara LT, Luber BS, Wang H et al. (2013). PD-L1 expression in the Merkel cell carcinoma microenvironment: association with inflammation, Merkel cell polyomavirus and overall survival. *Cancer Immunol Res*, *1* (1), 54-63.
- Liu W, MacDonald M, You J. (2016). Merkel cell polyomavirus infection and Merkel cell carcinoma. *Curr Opin Virol*, *20*, 20–7. doi: 10.1016/j.coviro.2016.07.011.
- Liu W, Wang X. (2019). Prediction of functional microRNA targets by integrative modeling of microRNA binding and target expression data. *Genome Biol*, *20*(1), 18. doi: 10.1186/s13059-019-1629-z.
- Mantel A, Carpenter-Mendini A, VanBuskirk J, Pentland AP. (2014). Aldo-keto reductase 1C3 is overexpressed in skin squamous cell carcinoma (SCC) and affects SCC growth via prostaglandin metabolism. *Exp Dermatol*, *23*(8), 573-8.
- Mantripragada K, Birnbaum A. (2015). Response to anti-PD-1 therapy in metastatic Merkel cell carcinoma metastatic to the heart and pancreas. *Cureus*, *7*(12), e403.

- Marcoval J, Mateo F, Palomero L, Badenas C, Piulats JM, Malvehy J, Pujana MA, Puig S, Fabra À. (2017). AURKA Overexpression Is Driven by FOXM1 and MAPK/ERK Activation in Melanoma Cells Harbouring BRAF or NRAS Mutations: Impact on Melanoma Prognosis and Therapy. *J Invest Dermatol*, *137*(6), 1297-1310.
- Marcoval J, Mateo F, Palomero L, Badenas C, Piulats JM, Malvehy J, Pujana MA,Puig S, Fabra À. (2017). AURKA Overexpression Is Driven by FOXM1 and MAPK/ERK Activation in Melanoma Cells Harboring BRAF or NRAS Mutations: Impact on Melanoma Prognosis and Therapy. *J Invest Dermatol*, *137*(6), 1297-1310.
- Mariot P, Vanoverberghe K, Lalevee N, Rossier MF & Prevarskaya N. (2002). Overexpression of an alpha 1H (CaV3.2) T-type calcium channel during neuroendocrine differentiation of human prostate cancer cells. *J. Biol. Chem*, *277*(13), 10824–10833.
- Marks F, Fürstenberger G & Müller-Decker K. (2007). Tumor promotion as a target of cancer prevention. *Recent Results Cancer Res*. *174*, 37–47.
- Marzban S, Geramizadeh B, Farzaneh MR. (2011). Merkel cell carcinoma in a 17-year-old boy, report of a highly aggressive fatal case and review of the literature. *Rare Tumors*. *3*(3), e34.
- Medina Franco H, Urist MM, Fiveash J, Heslin MJ, Bland KI, Beenken SW. (2001). Multimodality treatment of Merkel cell carcinoma: case series and literature review of 1024 cases. *Ann Surg Oncol*, *8* (3) , 204-208
- Melkamu T, Zhang X, Tan J, Zeng Y, and Kassie F. (2010). Alteration of microRNA expression in vinyl carbamate-induced mouse lung tumors and modulation by the chemo-preventive agent indole-3-carbinol. *Carcinogenesis*, *31*(2), 252–258.
- Mihailovic A, Morozov P, Brown M, Gogakos T, Mobin MB, Snorrason EL, Feilotter HE, Zhang X, Perlis CS, Wu H, Suárez-Fariñas M, Feng H, Shuda M, Moore PS, Tron VA, Chang Y, Tuschl T. (2013). Multicolor microRNA FISH effectively differentiates tumor types. *J Clin Invest*, *123*(6), 2694-702.
- Miller RW, Rabkin CS. (1999). Merkel cell carcinoma and melanoma: Etiological similarities and differences. *Cancer Epidemiol Biomark Prev Publ Am Assoc Cancer Res Cosponsored Am Soc Prevent Oncol*, *8*(2), 153–8.

- Mills LA, Durrani AJ, Watson JD. (2006). Merkel cell carcinoma in South East Scotland, 1993–2003. *Surgeon. 4*(3), 133–8.
- Monteith G R, Davis F M & Roberts-Thomson S J. (2012). Calcium channels and pumps in cancer: changes and consequences. *J. Biol. Chem*. *287*(38), 31666–31673.
- Moshiri AS, Doumani R, Yelistratova L, Blom A, Lachance K, Shinohara MM, et al. (2017). Polyomavirus-negative Merkel cell carcinoma: A more aggressive subtype based on analysis of 282 cases using multimodal tumor virus detection. *J Invest Dermatol, 137*(4), 819–27.
- Nardi V, Song Y, Santamaria-Barria JA, Cosper AK, Lam Q, Faber AC, et al. (2012). Activation of PI3K signaling in Merkel cell carcinoma. *Clin Cancer Res*, *18* (5), 1227-1236.
- Neumann F, Borchert S, Schmidt C, Reimer R, Hohenberg H, Fischer N, et al. (2011). Replication, gene expression and particle production by a consensus Merkel cell polyomavirus (MCPyV) genome. *PLoS One*, *6*(12), e29112.
- Ng L, Beer TW, Murray K. (2008). Vascular density has prognostic value in Merkel cell carcinoma. *Am J Dermatopathol*, *30* (5), 442-445.
- Nghiem PT, Bhatia S, Lipson EJ, Kudchadkar RR, Miller NJ, Annamalai L, et al. (2016). PD-1 blockade with Pembrolizumab in advanced Merkel-cell carcinoma. *N Engl J Med*, *374*(26), 2542–52.
- Paine E, Palmantier R, Akiyama S K, Olden K & Roberts J D. (2000). Arachidonic acid activates mitogen-activated protein (MAP) kinase-activated protein kinase 2 and mediates adhesion of a human breast carcinoma cell line to collagen type IV through a p38 MAP kinase-dependent pathway. *J. Biol. Chem*, *275*(15), 11284–11290.
- Panelos J, Batistatou A, Paglierani M, Zioga A, Maio V, Santi R, Pimpinelli N, De Giorgi V, Santucci M, Massi D. (2009). Expression of Notch-1 and alteration of the E-cadherin/beta-catenin cell adhesion complex are observed in primary cutaneous neuroendocrine carcinoma (Merkel cell carcinoma). *Mod Pathol*, *22*(7), 959-68
- Perrett CM, Walker SL, O'Donovan P, Warwick J, Harwood CA, Karran P, et al. (2008). Azathioprine treatment photosensitizes human skin to ultraviolet a

radiation. *Br J Dermatol*, *159*(1), 198–204.

- Pfeffer SR, Grossmann KF, Cassidy PB, Yang CH, Fan M, Kopelovich L, Leachman SA, Pfeffer LM.(2015). Detection of Exosomal miRNAs in the Plasma of Melanoma Patients. *J Clin Med*, *4*(12), 2012-27.
- Popp S, Waltering S, Herbst C, Moll I, Boukamp P. (2002). UV-B-type mutations and chromosomal imbalances indicate common pathways for the development of Merkel and skin squamous cell carcinomas. *Int J Cancer*, *99*(3), 352–60.
- Poulsen M. (2005). Merkel cell carcinoma of skin: diagnosis and management strategies. *Drugs Aging*, *22* (3), 219-229.
- Puig-Butille JA, Vinyals A, Ferreres JR, Aguilera P, Cabré E, Tell-Martí G,
- Renwick N, Cekan P, Masry PA, McGeary SE, Miller JB, Hafner M, Li Z,
- Riou-Gotta MO, Fournier E, Danzon A, Pelletier F, Levang J, Mermet I, et al. (2009). Rare skin cancer: A population-based cancer registry descriptive study of 151 consecutive cases diagnosed between 1980 and 2004. *Acta Oncol*, *48*(4), 605–9.
- Robertson JP, Liang ES, Martin RC. (2015). Epidemiology of Merkel cell carcinoma in New Zealand: A population-based study. *Br J Dermatol*, *173*(3), 835–7.
- Sarver AL, French AJ, Borralho PM et al. (2009). Human colon cancer profiles show differential microRNA expression depending on mismatch repair status and are characteristic of undifferentiated proliferative states. *BMC Cancer, 9*(401).
- Schadendorf D, Lebbe C, Zur Hausen A, et al. (2017). Merkel cell carcinoma: epidemiology, prognosis, therapy and unmet medical needs. *Eur J Cancer*, *71*, 53–69.
- Scuderi MR, Anfuso CD, Lupo G, Motta C, Romeo L, Guerra L, Cappellani A,Ragusa N, Cantarella G, Alberghina M. (2008). Expression of Ca (2+)-independent and Ca (2+)-dependent phospholipases A (2) and cyclooxygenases in human melanocytes and malignant melanoma cell lines. *Biochem Biophys Acta*. *1781*(10), 635-42.
- Scuderi MR, Anfuso CD, Lupo G, Motta C, Romeo L, Guerra L, Cappellani

A,Ragusa N, Cantarella G, Alberghina M. Expression of Ca(2+)-independent and Ca(2+)-dependent phospholipases A(2) and cyclooxygenases in human melanocytes and malignant melanoma cell lines. (2008). *Biochim Biophys Acta*, *1781*(10), 635-42.

- Sihto H, Kukko H, Koljonen V, Sankila R, Bohling T, Joensuu H. (2011). Merkel cell polyomavirus infection, large T antigen, retinoblastoma protein and outcome in Merkel cell carcinoma. *Clin Cancer Res Off J Am Assoc Cancer Res*, *17*(14), 4806–13.
- Smith VA, Camp ER, Lentsch EJ. (2012). Merkel cell carcinoma: identification of prognostic factors unique to tumors located in the head and neck based on analysis of SEER data. *Laryngoscope*, *122* (6), 1283-1290.
- Stetsenko GY, Malekirad J, Paulson KG, Iyer JG, Thibodeau RM, Nagase K et al. (2013) . p63 expression in Merkel cell carcinoma predicts poorer survival yet may have limited clinical utility. *Am J Clin Pathol*, *140* (6), 838-844.
- Swick BL, Srikantha R, Messingham KN. (2013). Specific analysis of KIT and PDGFR-alpha expression and mutational status in Merkel cell carcinoma. *J Cutan Pathol*, *40* (7), 623-630.
- Tadmor T, Aviv A, Polliack A. (2011). Merkel cell carcinoma, chronic lymphocytic leukemia and other lymphoproliferative disorders: An old bond with possible new viral ties. *Annal Oncol Off J Europ Soc Med Oncol/ESMO*, *22*(2), 250–6.
- Tang CK, Toker C. (1978). Trabecular carcinoma of the skin: an ultrastructural study. *Cancer*, *42*(5), 2311–21.
- Toker C. (1972). Trabecular carcinoma of the skin. *Arch Dermatol*, *105*(1), 107–10.
- Torchia EC, Chen Y, Sheng H, Katayama H, Fitzpatrick J, Brinkley WR, Caulin C, Sen S, Roop DR. (2009). A genetic variant of Aurora kinase A promotes genomic instability leading to highly malignant skin tumors. *Cancer Res*, *69*(18), 7207-15
- van der Zwan M, Trama A, Otter R, Larranaga N, Tavilla A, Marcos-Gragera R, et al. Rare neuroendocrine tumours: results of the surveillance of rare cancers in Europe project. *Eur J Cancer*, *49* (11) , 2565-2578.

- Van Gele M, Kaghad M, Leonard JH, Van Roy N, Naeyaert JM, Geerts ML, et al. (2000). Mutation analysis of P73 and TP53 in Merkel cell carcinoma. *Br J Cancer, 82*(4), 823–6.
- Walocko FM, Scheier BY, Harms PW, Fecher LA, Lao CD. (2016). Metastatic Merkel cell carcinoma response to nivolumab. *J Immunother Cancer*, *4*, 79.
- Wang D Z & Dubois RN. (2010). Eicosanoids and cancer. *Nat. Rev. Cancer*, *10*(3), 181–193.
- Wheat R, Roberts C, Waterboer T, Steele J, Marsden J, Steven N M & Blackbourn D J. (2014). Inflammatory cell distribution in primary merkel cell carcinoma. *Cancers, 6*(2), 1047–1064. doi:10.3390/cancers6021047.
- Wooff JC, Trites JR, Walsh NM, Bullock MJ. (2010). Complete spontaneous regression of metastatic merkel cell carcinoma: A case report and review of the literature. *Am J Dermatopathol, 32*(3), 614–617.
- Xie H, Lee L, Caramuta S, Hoog A, Browaldh N, Bjornhagen V, Larsson C, Lui WO. (2014). MicroRNA expression patterns related to merkel cell polyomavirus infection in human merkel cell carcinoma. *J. Investig. Dermatol*, 134(2), 507–517. doi: 10.1038/jid.2013.355.
- Youlden DR, Soyer HP, Youl PH, Fritschi L, Baade PD. (2014). Incidence and survival for Merkel cell carcinoma in Queensland, Australia, 1993-2010. *JAMA Dermatol, 150*(8), 864–72.
- Zhao Q, Deng S, Wang G, Liu C, Meng L, Qiao S, Shen L, Zhang Y, Lü J, Li W,Zhang Y, Wang M, Pestell RG, Liang C, Yu Z.(2016). A direct quantification method for measuring plasma MicroRNAs identified potential biomarkers for detecting metastatic breast cancer. *Oncotarget*, *7*(16), 21865-74. doi:10.18632/oncotarget.7990.
- Zhu H. et al. (2014). Elevated Orai1 expression mediates tumor-promoting intracellular Ca2+ oscillations in human esophageal squamous cell carcinoma. *Oncotarget, 5*(11), 3455–3471.